Estimating mobility values from electroluminescence measurements on organic polymers

by

Judith Andrea Castelino

Submitted to the Department of Electrical Engineering and Computer Science
in partial fulfillment of the requirements for the degree of

Master of Engineering in Electrical Engineering

at the

MASSACHUSETTS INSTITUTE OF TECHNOLOGY

September 1995

Author .....
Department of Electrical Engineering and Computer Science
Aug 21 1995

Certified by .....
Mildred Dresselhaus
Professor
Thesis Supervisor

Accepted by .....
F. R. Morgenthaler
Chairman, Departmental Committee on Graduate Students

Estimating mobility values from electroluminescence measurements on organic polymers

by

Judith Andrea Castelino

Submitted to the Department of Electrical Engineering and Computer Science
on Aug 21 1995, in partial fulfillment of the
requirements for the degree of
Master of Engineering in Electrical Engineering

Abstract

The use of polyphenyl vinylene in organic light emitting diodes has been motivated by its high luminosity yield and its low temperature manufacturing. The luminosity yield is limited by the rate at which charge can be injected into the sample. Yan et al. (1994) suggest that using amorphous PPV instead of polycrystalline PPV as is conventionally used should increase the luminosity yield. Amorphous PPV is achieved by including a large number of cis inclusions, which prevent crystal formation. A side effect of cis inclusions is that the effective conjugation length of the molecules is shortened.

This thesis repeats mobility measurements done on conventional PPV, using amorphous PPV. We find that the mobility is decreased by 1-2 orders of magnitude, and that the average conjugation length is not a limiting factor to the mobility. While the luminosity yields are high, the current voltage traces indicate that the devices are space charge limited and that this limits the luminosity yields.

Thesis Supervisor: Mildred Dresselhaus
Title: Professor

Acknowledgments

I would like to thank Mildred Dresselhaus for her support and advice throughout this thesis, for all of the attention to details, and for all of the corrections from which this thesis has benefitted. I am grateful for the guidance and all she has taught me about writing a scientific document. I would like to thank Lewis Rothberg, for his support with the experimental work, for his help with the writing of the document, and for his confidence in me. Lastly, I would like to thank Alex Fung, for helpful advice, for his generosity with his time and for a lot of attention to detail in my experimental work. I learnt a lot from my experience with this thesis, and I am grateful for all of the help I received, and to all of the people without whom this thesis would not have been possible. Thank you.

Contents

List of Figures

List of Tables

Chapter 1

Introduction

A growing research area is the use of organic polymers as active materials in transistor and Light Emitting Diode (LED) technologies. The response time and current carrying capacity of these devices depends on the mobility and the dispersion in the velocities of charge carriers as they move through the sample. In order to optimally exploit applications of organics in devices, these transport properties must be studied and understood.

Conjugated polymers have at least one unsaturated bond. The electrons in this bond are located in π-orbitals and are free to transport charged particles. The transport of carriers is usually along these bonds, with carriers hopping between the π-bonds of different molecules. The transit time across the sample is limited by the speed with which the carriers can hop between orbitals.

Transport properties of organics are complicated by the irregular packing structure of the molecules (i.e., disorder). Molecules can form complex cross linkages which affect the transport properties. The transport properties will also be affected by defects in the sample and the presence of crystallite grain boundaries. The effects of morphology on transport properties can be studied using x-ray diffraction techniques to examine the structure of the material. Alternatively, different sample preparation techniques, which are known to affect crystal size, can be used, or defects can be artificially introduced into the crystal structure.

1.1 Applications

Display technology for present lap top computers or projection displays is a fast growing industry. Cathode ray oscilloscope tubes (CRTs) which are used in televisions are not suitable for either of the above applications. CRT's are large and heavy, making them unsuitable for portable devices, and the thickness of the screen and the size of the cathode ray tube scale with screen size, making the CRTs extremely expensive for projection displays.

1.1.1 Thin Film Transistors

Liquid Crystal Displays (LCDs) are being used for lap top computers, and the use of similar technology is being investigated for projection displays.

Liquid crystals have a helical structure which rotates the plane of polarized light. When viewed between cross polarizers, the liquid crystals will be transmissive if the molecules are all aligned, or opaque if they are not. Liquid crystals can be aligned by applying a potential across the molecule.

The displays require the ability to switch each pixel individually in an array of 480×650 pixels.. Since it is not possible to make contact to each pixel individually, a variety of addressing schemes are being used. The simplest such scheme, passive addressing, is to switch a pixel by applying a half the switching voltage to the horizontal strip containing the pixel, and half the voltage to the vertical strip. The problem is that there are a number of pixels which have half the voltage applied to them, and appear grey. In addition, since the voltages required to switch the LCDs are on the order of Volts, the scheme requires large amplitude signals.

For this reason, Thin Film Transistors (TFTs) are used in the displays (active addressing). These transistors enable sending lower amplitude signals and eliminating the occurrence of grey pixels. TFTs are presently made of amorphous silicon evaporated onto a glass substrate. Plastics screens are not compatible with the fabrication method since they cannot be heated to the temperatures needed to make high quality amorphous silicon. Using glass in the screen makes the screen heavier, more inflexible

and more expensive. Currently the screen accounts for 70% of the cost and about 2/3 of the weight of a lap top computer.

One important application of organic polymers may be as TFT materials in lap top displays. Polymers can be spincoated onto the screen at low temperature, in a process compatible with plastic substrates for displays. This is one critical application for which it is desirable to study and improve the transport properties of organics.

1.1.2 Light Emitting Diodes

Organic polymers are also being used as the active layer in light emitting diodes (LEDs). The diodes can be manufactured on plastic substrates, making them more strain resistant, and more suitable for large displays. The use of organic diodes in flat panel emissive displays is therefore being investigated.

Organic polymers are well suited to display applications, since the application does not place stringent requirements on the speed of the devices. However, although the response times of organic devices are fast enough for display purposes, the low mobility limits the rate at which charge can be injected into the devices, and hence the intensity with which the device emits light.

1.2 Background

1.2.1 LEDs

The use of organics as the active layer in light emitting diodes was first demonstrated in the 1960's when electroluminescence was observed in crystalline anthracene [10]. The devices were not of practical interest because of the high threshold voltages and the low external quantum efficiency of the devices. Even after work was done to lower the threshold voltages, the unstable structure of the organic made its use in an active element impractical.

The first realisable organic diode was presented nearly twenty years later, when electroluminescence was observed in organic dye molecules which were diffused through

a polymer matrix.

201z In 1990, Burroughes et al. [5] presented a polyphenyl vinylene (PPV) diode that showed that polymers which could be easily spun from solution could be used as electroluminescent devices. Although the efficiency of the devices was low, there was hope that changes in the manufacturing process and addition of different side groups, which would change the packing structure, could produce a commercially viable product.

Currently most of the work has been in PPV and related derivatives. PPV, however, has a fairly low mobility and improved charge transport is desirable to achieve power efficient enhancements.

1.2.2 Thin Film Transistors (TFTs)

Research in organic polymers for TFT applications has also focused heavily on conjugated polymers. A second material being studied for the use in transistors is alpha hexathiophene ($\alpha - 6T$). Mobilities on the order of $10^{-2}cm^2/Vs$ are being reported in this material, in comparison to mobilities of $10^{-1}cm^2/Vs$ for amorphous silicon.

Morphological studies of $\alpha - 6T$ have also shown that the molecules align in a regular structure, meaning that the measured mobility will not be as strongly influenced by the presence of defects, and will be closer to the intrinsic mobility of the organic materials.

The performance of TFTs is also limited by transport and low mobility values. Low mobilities lower the response time of the devices.

1.3 Motivation

The compatibility if organic polymers with plastic substrates has distinguished them for use in display technology. The use of organic semiconductors is however delayed by the low mobilities which are reported for these materials. Low mobilities lengthen the response time and current carrying capacity of TFTs and lower the power efficiency of LEDs because of space charge limited injection. In order to improve device

specifications, it is necessary to measure mobility profiles, and to understand the processes which limit mobilities.

This thesis attempts to do this by developing a technique for measurement of mobility based on transient electroluminescence. The technique is general to emissive organics. The mobility profiles of polyphenyl vinylene (PPV) and various chemical modifications of it are measured. The effects of the modifications on mobility are studied.

Chapter 2

Transport Properties

Conjugated polymers consist in general of repeated units of simple organic monomers, with alternating single and double bonds[11]. The electrons about each carbon atom are split into two sp^2 hybridized orbitals which contain a total of six electrons, and p_z orbitals which contain a total of two electrons, and are half filled. The sp^2 orbitals are oriented in a planar configuration, and the p_z orbitals are oriented perpendicular to the plane.

The simplest conjugated polymer, polyacetylene, is made up of repeated units of ethene. Polyacetylene consists of a chain of carbon atoms with alternating single and double bonds.

The electrons in the p_z orbitals form the π-electrons which are responsible for conduction. In polyacetylene, the p_z orbitals will hybridize in order to lift the degeneracy and to lower the ground state energy of the molecule[11]. The p_z orbitals form two new orbitals, a π orbital and a π^* orbital, separated by an energy gap. Depending on the position of the Fermi level of the molecule relative to the energy gap, the molecule will be either a semiconductor or an insulator.

In more complicated polymers, the π orbitals gets split into many different bands. The term π orbital then refers to the highest occupied molecular orbital (HOMO). Typical polymers used as organic semiconductors may consist of benzene rings with side chains. Poly Phenyl Vinylene (PPV), which is the polymer we use in this thesis, consists of repeated links of Benzene with an ethene side chain (see fig 2-1).

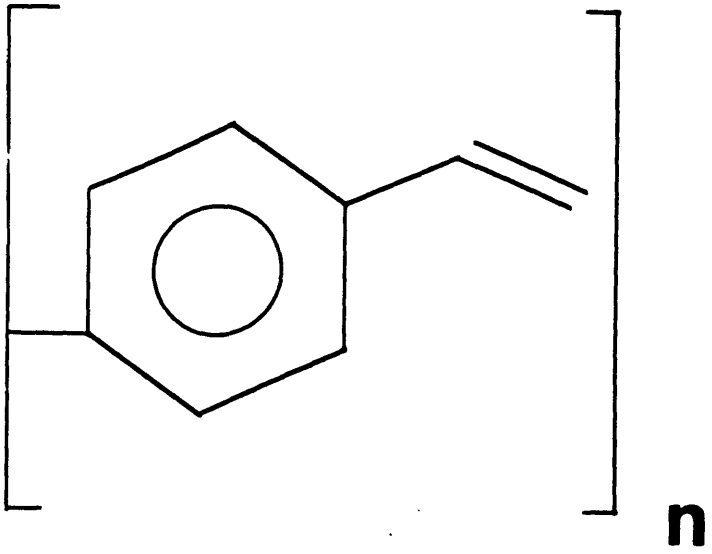

Figure 2-1: Structure of Poly Phenyl Vinylene(PPV)

2.1 Transport Mechanisms - Silicon

Organic semiconductors, in general have lower mobilities than inorganic semiconductors. This is due in part to the higher levels of defects and impurities in the polymer films, but also to the disorder in the structure of the molecules. The disordered structure means that the overlap integral is smaller, and hence the bandwidths of the molecular orbitals are on the order of the thermal energy of the carriers [6]. This lowers the mobility.

Carriers in inorganic semiconductors travel by means of band transport. Because of the regular structure of the silicon atoms in the crystal, the electronic orbitals of the atoms overlap, and form an electronic band, in which carriers are free to travel.

Electrons get thermally excited from the filled valence band to the unfilled conduction band. This leaves a positively charged hole in the valence band, and a negatively charged electron in the conduction band. Since the bands are unfilled, both electron and hole carriers are free to travel in the bands, and transport occurs within the semiconductor. The number of conducting carriers follow a thermally activated

distribution

$$n = n_0 e^{-E_a/kT},$$

where E_a is the activation energy which is the difference between the Fermi energy of the carrier and the energy level of the conduction band.

Once excited into the conduction band, the carriers are free to move within these bands since the bands are not filled. The carriers drift under the influence of an electric field according to

$$v = \mu E.$$

where the mobility, μ, is constant for low voltages.

Because of the irregular structure of organics, the molecules will not be packed as closely. There will be less overlap between wavefunctions, and the orbitals do not form bands, but rather the π orbitals are localized and confined to individual molecules.

2.2 Transport Mechanisms

Transport in organics occurs in the π orbitals[11]. Electrons in these orbitals are not localized on any carbon atom since the π orbitals are spread across the molecule. Electrons are free to move across the molecule, and carrier transport occurs as electrons hop from one polymer molecule to the next.

The double bond in the conjugated polymers is rigid, meaning that the carbon atoms are not allowed to rotate about their positions in the chain. The double bond also prevents bending and twisting motion since the deformation energy of the molecule is high. The molecules form quasi one dimensional structures because of this, with transport mechanisms characteristic of one dimensional molecules.

The electron-phonon interaction in one dimensional molecules is generally higher than in three dimensional molecules[6]. Because of this, a charge carrier will deform the lattice about it. The charge carrier and the lattice deformation will move together and form a quasi particle known as a polaron. The polaron will have the same charge

as an electron.

The energy gained from the deformation of the lattice, moves two electron states, one above and one below the band gap into the band gap. In doing so, the deformation lowers the ground state energy of the electron. This also effectively lowers the band gap of the organic molecule. The formation of polarons follows a thermally-activated distribution

$$n = n_0 e^{-E_A/kT}.$$

where E_A is the activation energy needed to form the polaron.

In the case of organic polymers, the velocity of the carriers is limited not by the time needed to form the polaron, but by the time needed for the polaron to move between the orbitals of different molecules. Various transport mechanisms have been proposed, amongst them variable range hopping, constant length hopping, quantum mechanical tunneling, etc. Tunneling transport occurs when carriers tunnel between defects in the sample (see fig 2-2). Hopping occurs when carriers are thermally excited out of the traps into the molecular orbitals where transport can occur. Experiments suggest that transport within the sample occurs through hopping [20].

The hopping mechanism in polyphenyl vinylene is best described by variable range hopping, where the distance which the carrier moves is variable. The temperature dependence of this mechanism goes as

$$\mu(T) = \mu_0 e^{-(T_0/T)^\alpha},$$

where μ is the mobility, T_0 is a measure of the energy needed to hop between polymer molecules, and α has a values between 1/2 and 1/4 [18].

2.3 Trapping

Carrier transport in organics is also limited by the presence of trapping sites. Organic polymers contain enough traps so that the time spent travelling between traps is negligible compared to the time spent in the traps[12, 18]. The motion of carriers

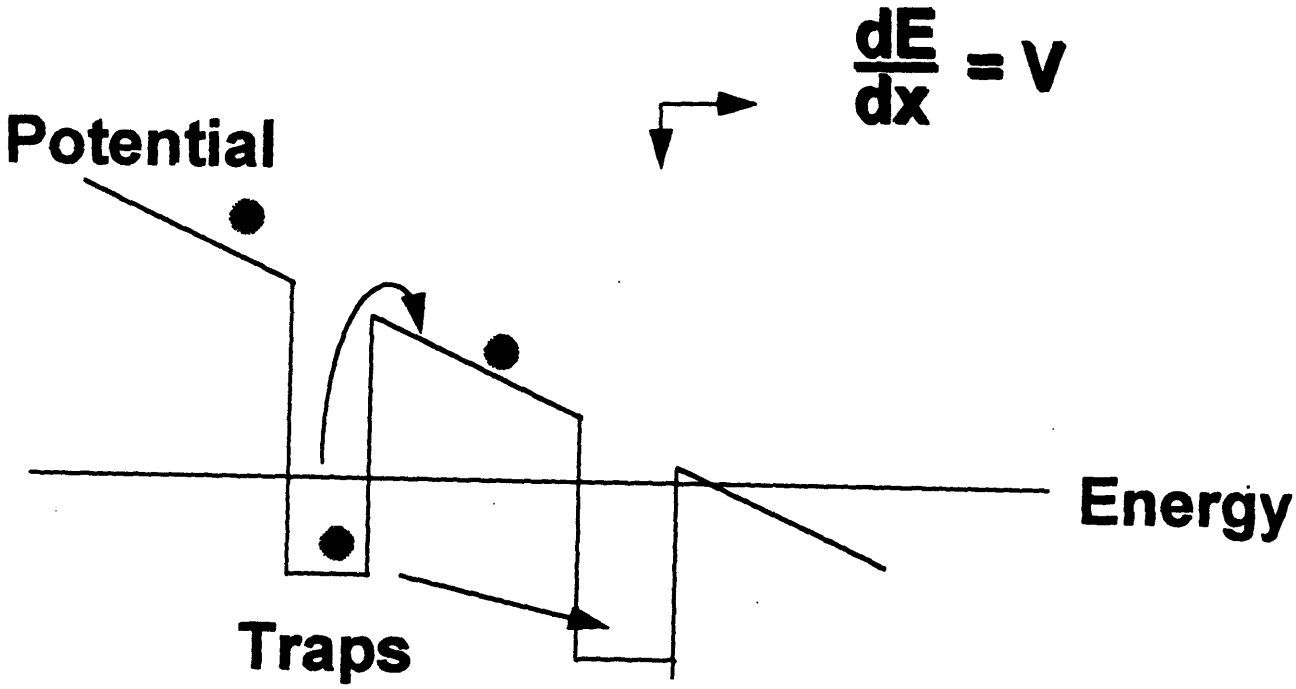

Figure 2-2: Hopping vs. Tunneling Transport
The energy levels of the molecular orbits are disrupted by trapping sites. Since PPV is a disordered systems, these traps will have variable width, depth and separation. An applied electric field is equivalent to tilting the energy levels of the orbitals. At low applied fields, carriers will hop out of traps. The hopping mechanism is not confined to hopping between neighboring trapping sites, since depending on the applied potential, a carrier may gain more energy by hopping over multiple trapping sites.

across the sample can be thought of as a three dimensional random walk with carriers hopping from one trapping site to the next.

The time taken for a carrier to detrap from a trapping site follows a thermally activated pattern

$$\tau = \tau_0 e^{-E_a/kT},$$

with the mean detrapping time, τ, following an exponential distribution according to the activation energy E_a. Since the detrapping time has some distribution and since the time depends on the depth of the trap, which itself has some distribution, the motion can be treated as a random walk with variable time between steps.

The distance travelled between hops is also randomly distributed, since the traps are randomly distributed. The motion is best described by variable range hopping. The distribution in time between steps can be incorporated into the model as a distribution in the step size of the random walk. The temperature dependence of variable range hopping is given by

$$\tau = \tau_0 e^{-(T_0/T)^\alpha} \quad , \quad \alpha = 1/2 \ldots 1/4 \tag{2.1}$$

where τ is the mean detrapping time and kT_0 is a characteristic energy about which the trap depths are distributed. We can then introduce $P(\tau)$ as the probability that the carriers escape in τ seconds.

2.4 Hopping Mechanisms

Organics contain a large concentration of trapping sites, with a distribution of different trap depths (see Fig. 2-2). For analytic purposes, the traps can be divided according to trap depth into traps from which the carriers will on average escape on the time scale of the experiment and traps from which the carrier will not escape on the time scale of the experiment. In this experiment, the time scale is the time between repetitions of the electric pulse.

The distribution of shallow trap depths will give rise to a dispersion in the velocity

profile, since the traps limit the hopping velocity. Scherr and Montroll derived an expression for the velocity profiles which result from a single trap depth, and from an exponential distribution of trapping depths [18]. They find that their predictions agree well with data taken from time of flight measurements on samples with a sandwich geometry [1, 17]

The distribution in deep traps will give rise to permanent trapping, and an attenuation of the signal. Balagurov and Vaks treat trapping mechanisms in organics as hard sphere scattering off the trapping sites and obtain an expression for the number of carriers $n(t)$ as a function of time, where t is set by the time since injection [3]

$$n(t) = n(0)e^{-ct^{1/2}}$$

This "permanent trapping" also results in an offset from the dark current level in the dc level of the signal, as trapped electrons are constantly detrapping.

2.4.1 Field Dependence

The electric fields being applied to the sample are too small to affect the velocity due to scattering, $dE << U_t$, where d is the lattice constant and U_t is the trap depth. However, since the trap concentration is high, $lE > U_t$, where l is the mean free path between trapping sites, and E is the electric field. As a result of this, the detrapping times will be field dependent,

$$\tau = \tau_0 e^{[-(qV-U_t)/kT]^{\alpha}}.$$

In cases where the trap density is not as high, and the relation $lE < U_t$ is valid, the applied field is unlikely to result in shorter detrapping times. The field dependence of the transit time is therefore likely to be due to a velocity dependent trapping cross section.

The carriers are accelerated by the field, E. Since the distance between traps is small, the carriers will not reach terminal velocity within the sample. Terminal

velocity for the sample is determined by scattering off a perfect defect-free lattice, and is field independent. The velocity dependence of the trapping potential can be treated as hard sphere scattering with a field dependent impact parameter.

2.4.2 Trapping Mechanisms

The traps in organics give rise to a dispersive velocity profile, and an exponential tail to the transit time distribution as the "permanently trapped" carriers detrap. The decay constant in the exponential tail, and the temperature dependence of the transit times of the carriers will give an indication of the dominant trap depths, assuming there are any.

Traps in organics can result from several things. Grain boundaries of crystals, defects in the organic material, or cross linkages between different polymer molecules. The effects of these trapping mechanisms can be studied by artificially introducing extra traps, for example by changing annealing conditions, which change the size of the crystallites or by introducing defects into the sample.

Another trapping mechanism may be hopping between the π orbitals of different molecules. If the molecules had some ordered alignment, then the energy needed to hop between molecules may be some fixed level. In the case of many of the organics being used, it is likely that this is the case since the molecules are fairly rigid. The mobility associated with the carriers hopping between the different π orbitals is an important parameter, since it represents the intrinsic mobility of the sample. The intrinsic mobility can be changed by attaching different side groups to the molecules, which will change the way the molecules pack, and possibly lower the threshold energy needed to hop.

2.4.3 Trap Depths

Since the energy level of the electrons in the contact lies in the band gap of the organic, an activation energy is needed to move carriers into the π and π^* orbitals. The band gap is about 2 eV and the energy between the Highest Occupied Molecular

Orbital and the energy of a hole at the Fermi level is on the order of 0.1 Volt. The number of carriers in the sample will follow a thermally activated distribution with the temperature dependence given by eq 2.2.

$$n(T) = n_0 e^{-E_a/kT} \tag{2.2}$$

Because the carriers need this energy in order to enter the π orbitals, trapping on energy scales less than 0.1 eV will not be distinguishable from our current-voltage profiles. This further restricts the scales which we are considering to 0.1-1.3 eV for shallow traps and 1.3 - eV for deep traps, where 1.3 eV is the trap depth from which on average half of the carriers will detrap in the time between voltage pulses.

2.5 Molecular Orientation

In this thesis we examine the effect of varying the proportion of cis-connected monomers. Cis-connected monomers are those where the two neighboring phenyl rings are on the same side of the double bond (see fig 2-3). The phenyl rings are not free to rotate about the double bond which is rigid.

The proportion of cis vs trans monomers can be controlled in the polymerization stage, when the precursor is converted to polymer. The molecules are made with mostly trans linkages, and changing the number of cis linkages has the effect of changing the conjugation length of the trans connected regions. If the energy levels of the carrier are treated as that of a particle localized on the chain, then the energy levels can be approximated by those of a particle in a box, with longer conjugation lengths having lower energy states. Since the energy level separations are smaller, it will be easier for electrons to hop to the excited state of the molecule and to hop between molecular orbitals of different molecules. In cases where the transport is limited by the intrinsic mobility, that is hopping between different orbitals, rather than detrapping from defect sites, longer conjugation lengths also means fewer hops are necessary. Increasing the conjugation length should therefore increase the carrier

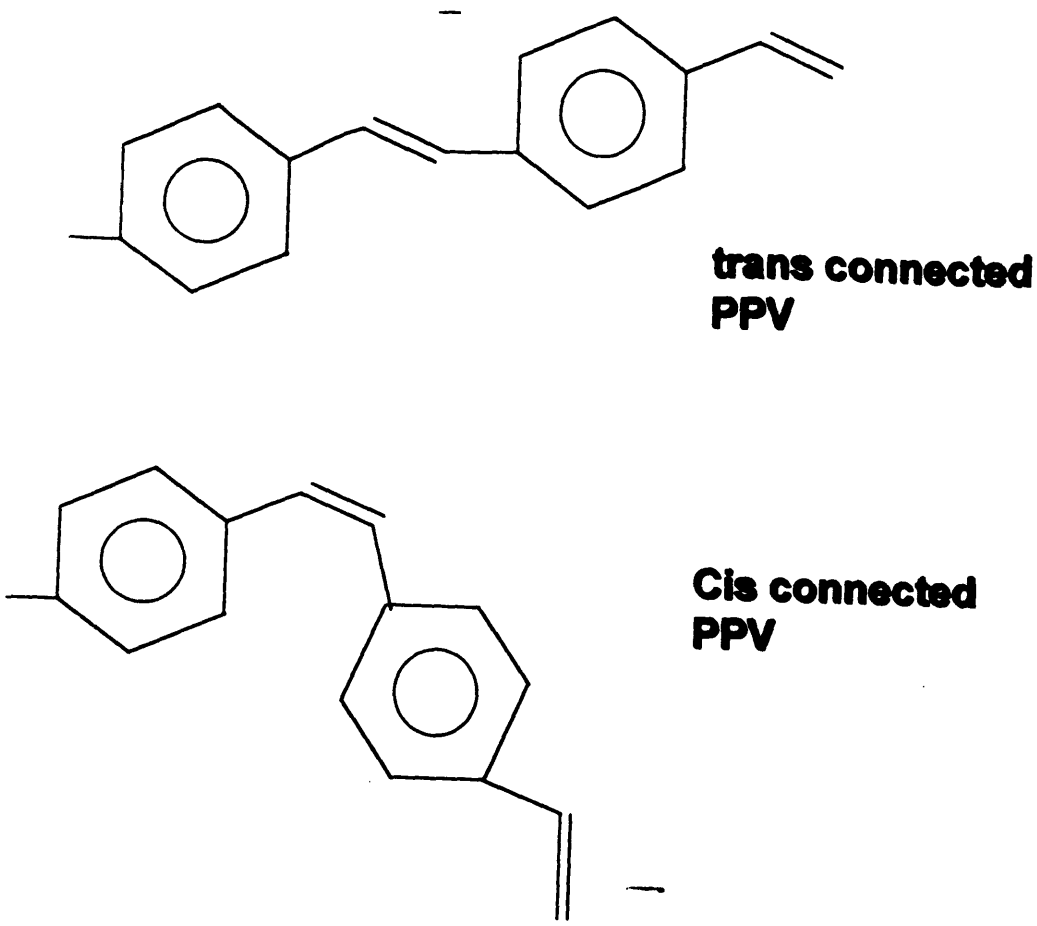

Figure 2-3: cis vs. trans polymers
Cis connected conjugation links have the phenyl rings on the same side of the double bond. Since the phenyl rings are bulky, they prevent the formation of a crystal lattice. Trans connected conjugation links have the phenyl rings on opposite sides of the double bond. Trans connected links remain straight and promote crystallization.

mobility.

Because the phenyl rings are bulky, having a cis linkage will reduce the efficiency with which molecules can pack, resulting in an amorphous polymer film. Molecules with cis linkages are more likely to form cross linkages than molecules without cis linkages, which is equivalent to having more trapping sites for the cis-linked segments.

In samples where there is a substantial fraction of cis linkages, the electronic wavefunctions will also have less overlap, meaning that it will be harder for electrons to hop from one molecule to the next.

Chapter 3

Device Characteristics

The aim of the experiment is to use electroluminescence data to measure the distribution in mobilities of carriers in samples of PPV. The samples consist of a layer of polymer between a transparent Indium Tin Oxide (ITO) electrode and a metal electrode.

The electrons in the sample have low mobilities and remain fixed at the metal electrode. Holes are injected at the ITO contact, and travel towards the metal contact, where the electrons are located. The holes and electrons form excitons, bound hole-electron pairs, and subsequently recombine, emitting light. The time taken for the exciton to radiate is much shorter (1 ns) than the time taken to travel across the sample, and can be neglected.

From the distribution in transit times, we extract the carrier mobilities and attempt to extract information about the distribution of trap depths in the sample. The analysis is repeated on samples with a higher proportion of cis linkages, to see whether this parameter affects the mobility.

3.1 Charge Distribution

When two metals with different work functions are brought into contact with each other, a built in potential difference develops across the junction[14. 20]. If an insulator is inserted between the two metals, a uniform electric field develops across the

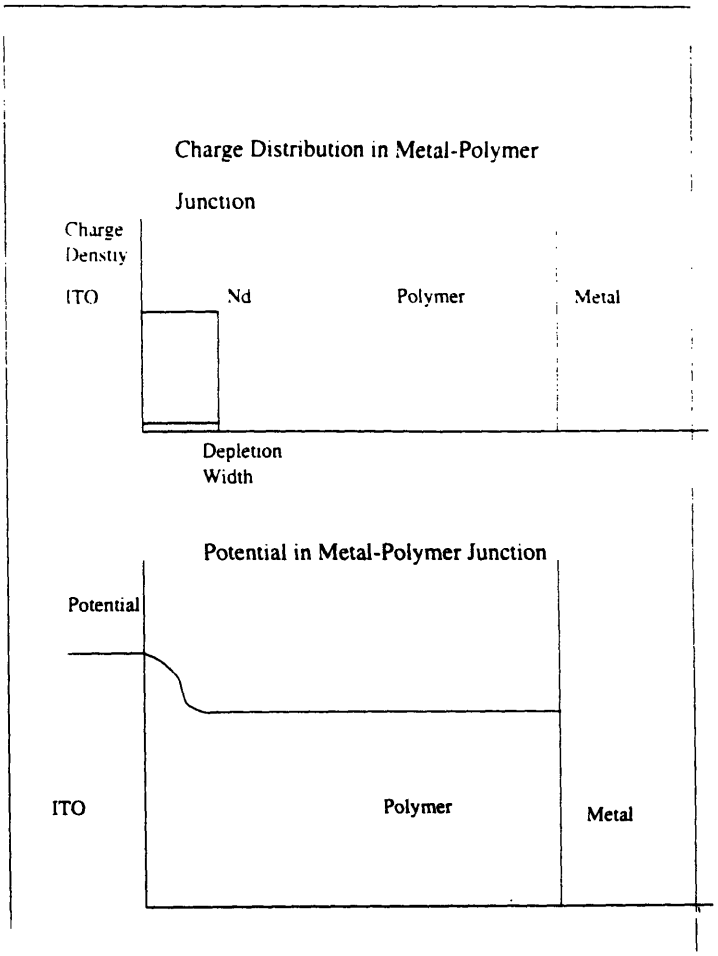

Figure 3-1: Potential in a Metal-Semiconductor-Metal configuration
The depletion layer builds up as positively charged holes are repelled from the positive electrode. The depletion of charges from this region causes the potential profile shown above. The net density of charge is N_d, where N_d is the density of holes in the polymer.

insulator.

If a semiconductor is inserted between the two metal contacts, the carriers in the semiconductor are mobile and will migrate in order to shield the bulk of the semiconductor from the electric field. In organic polymers, which are in general p-type semiconductors, the holes will migrate to the negative metal electrode. A depletion layer will build up about the electrode. The charge distribution is shown in figure 3-1.

The charge distribution at the metal-semiconductor interface can be analysed using the depletion approximation for the semiconductor. According to this approxi-

mation, the charge density will be N_d in the bulk of the sample and 0 in the depletion layer. Since the electrons in the metal have high mobility compared to the electrons in the semiconductor, the excess charge on the metal side is located as a surface charge density at the interface.

Under equilibrium conditions, when no voltage is applied, no net current flows across the junction. The width of the depletion layer is such that the drift current caused by the potential across the junction exactly cancels the diffusion current due to the depletion of holes at the electrode. The potential at the junction will change as a result of the build-up in charged carriers. Assuming a one dimensional junction, the electric field E becomes

$$E = \int dx qp/\epsilon + \Phi_{ITO}, \tag{3.1}$$

where x is the distance from the ITO electrode. Equating the drift and diffusion currents, j_{drift} and j_{diff} respectively, we obtain:

$$\begin{aligned} j_{drift} &= qp\mu_h & (3.2)\\ &= qD\frac{dp}{dx} = j_{diff}, & (3.3) \end{aligned}$$

where p is the density of holes, and D is the diffusion constant. Using the relation

$$D/\mu = kT/q, \tag{3.4}$$

equation 3-3 can be integrated to yield a depletion width [20],

$$w = \sqrt{\frac{2\epsilon}{N_d q}\left(\Phi - \frac{kT}{q}\right)}. \tag{3.5}$$

For a carrier density N_d of $10^{16}cm^{-3}$, and a dielectric constant ϵ of $3\times10^{-13}Farads/cm$, which is typical of organic semiconductors, the depletion width will be $100\mathring{A}$, compared to a sample thickness of $1000\mathring{A}$.

3.2 Electrical Properties

The long time needed to build up the depletion layer implies that the sample has a large capacitance. The capacitance of the sample is important for time resolution, since the time required for the voltage across the junction to change limits the response time of the sample. The capacitance is also important, since it gives a measure of the carrier density in the sample.

Given the charge profile of equation 3-5, the capacitance associated with the sample is

$$C = \epsilon A/d = 1200pF,$$

for a carrier density of $10^{16}cm^{-3}$.

The built-in potential of the junction and the area of the device are known, and the density of carriers in the organic material can be calculated to be [20]

$$N_d = -\frac{2}{q\epsilon}\frac{V - \Phi - \frac{kT}{q}}{C^2}, \tag{3.6}$$

where N_d is the concentration of holes when a voltage pulse V is applied.

3.2.1 Voltage

When a voltage is applied across the junction, the carriers will no longer be in equilibrium, and a current will flow across the junction. The magnitude of the current in the bulk of the sample will be the drift current due to the applied electric field,

$$j_{total} = j_{drift} = n\mu_h E \tag{3.7}$$

Assuming that carrier generation and recombination is negligible away from the electrodes, and that the depletion region is small compared to the bulk of the sample, the current flowing in the bulk of the sample will be the same as the current flowing across the depletion region.

Far away from the depletion region, the diffusion current will be zero. At the depletion region, the net current is

$$j_{diff} + j_{drift} = j_{total} = \mu_h q E.$$

The thickness of the depletion region will change as a result of the applied field. Following eq 3-5, the width of the depletion region now becomes

$$w = \sqrt{\frac{2\epsilon}{N_d q}\left(\Phi - V - \frac{kT}{q}\right)}. \tag{3.8}$$

3.3 Carrier Injection

3.3.1 Thermionic Injection

In a conventional semiconductor device, the charge is injected into the sample at the contacts by thermionic injection. The amount of charge injected into the junction can be determined by solving the equations for the drift and diffusion currents

$$\begin{aligned} j_{drift} &= j_{diff} \\ D_h \frac{dn}{dx} &= \mu n E. \end{aligned} \tag{3.9}$$

Using the relations

$$\begin{aligned} \frac{D_h}{\mu_h} &= \frac{kT}{q} \\ \int E dx &= V, \end{aligned} \tag{3.10}$$

this gives a solution

$$j = j_0\left(e^{qV/kT} - 1\right) \tag{3.11}$$

This is the equation for charge flow across a metal-semiconductor junction as a function of applied voltage.

The charge flow equation can be understood in terms of a band model [2]. The electrons need an activation energy E_a to be excited to the conduction band. In the presence of an applied potential V, the energy required to reach the conduction band is decreased.

3.3.2 Space Charge Limited Injection

If the mobility of the sample is low, then the charge injection will be limited by the rate at which the charge can be carried away from the junction. This is known as space charge limited injection.

If the carriers cannot be transported away from the junction fast enough, a layer of space charge will build up at the junction. The potential due to this charge will repel any additional carriers, and will lower the amount of charge injected into the junction.

The current flowing across the junction will be

$$j = \mu q \rho E,$$

where ρ is the space charge density and is proportional to $\frac{dE}{dx}$, and hence is proportional to E/d. The analytic derivation gives a current-voltage relationship, [20]

$$j = \frac{8\mu\epsilon}{9}\frac{V^2}{d^3} \tag{3.12}$$

for space charge limited injection.

This type of injection is particularly important for organic LEDs since there may be more trapping sites near the metal interface where the carriers may undergo nonradiative recombination. Having a large amount of the injected charge trapped at the interface may increase the rate of nonradiative recombinations [4], and lower light emission levels.

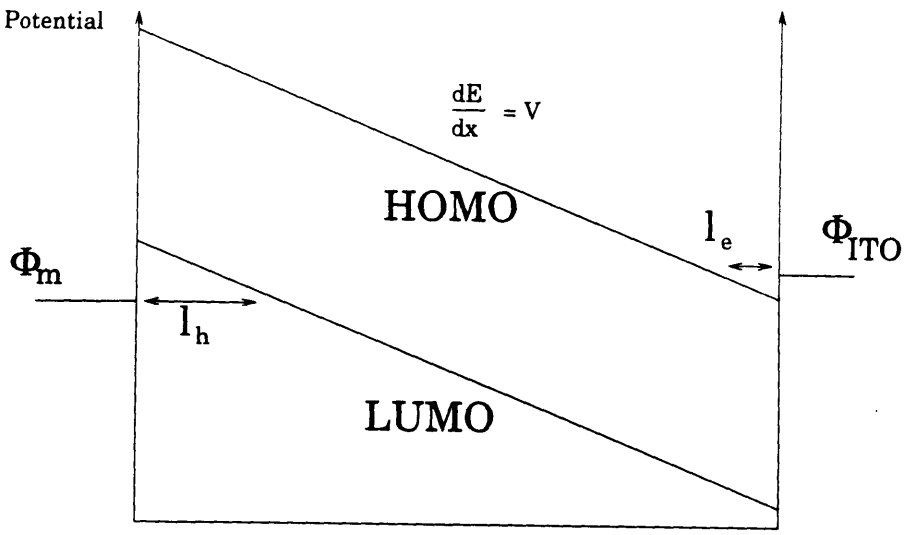

Figure 3-2: Band Levels for Tunneling Currents
In tunneling transport, the distance the carrier must tunnel depends on the electric field and the "tilt" of the energy levels of the molecular orbitals.

3.3.3 Tunneling Current

In metal-polymer junctions, there is evidence that carrier injection occurs as carriers tunnel into the junction (Fowler-Nordheim tunneling) [9]. The tunneling probability goes as [20]

$$j = e^{-kl},$$

where k is the wave vector of the electronic wave and l is the distance across which the electron tunnels.

The band structure model that accounts for this mechanism (Fowler-Nordheim Model) is given in figure 3-2. The ITO contact has a work function of 4.7 eV, and

the metal has a work function of around 4 eV, depending on the metal. The energy level of the Highest Occupied Molecular Orbits (HOMO) and Lowest Unoccupied Molecular Orbits (LUMO) are "tilted" as a result of the applied field. The injection rate into these devices depends on E rather than V, since the distance the carrier has to tunnel is proportional to $\Delta\Phi/E$. The Fowler-Nordheim Model predicts a tunneling current of

$$j = \kappa_1 E^2 e^{-\kappa_2/E}, \tag{3.13}$$

where κ_1 and κ_2 are constants, with dimensions of $ma - cm^2/V^2$ and V/cm respectively. Because the work function of the ITO is closer to the HOMO level than the work function of the metal is to the LUMO level, the carriers that are injected are predominantly holes.

3.3.4 Contact Potential

The level of injection which can be achieved will depend on the difference between the contact potentials of the metal electrodes, Φ_b [9]. The tunneling current is proportional to e^{-kl}, where $k = 4/3\sqrt{2m^*/h^2 q\Phi_b}$ and $l = \Phi_b/E$. So the injected charge is proportional to $e^{-(\Phi_b/\Phi_0)^{3/2}}$.

By varying the potentials of the positive and negative electrodes with respect to the energy levels of the molecular orbitals, it is possible to control the ratio of injected holes to injected electrons. It is advantageous to have more holes injected than electrons, since the holes in PPV have higher mobilities than the electrons. There is evidence [4] that this may be due to electron trapping sites, for example oxide molecules, which lower the electron mobility.

We chose to use Aluminum as the positive electrode and ITO as the negative electrode. By doing this, we achieved a device where the carriers were predominantly holes, and with a relatively high injection rate, since Aluminum has a high work function (4.75 eV), so the potential difference, Φ_b is small.

3.4 Device preparation

The samples are prepared by etching lines off an ITO coated slide. The glass substrate is cleaned and photoresist is spincoated onto the ITO covered side. The photoresist is baked, and the pattern is developed by exposing the photoresist to 100 Watts of UV light for 15 seconds. The ITO is etched off using concentrated HCl. The ITO is patterned into 4 mm wide strips.

PPV precursor is spun onto the patterned substrate. The precursor film is spun on at room temperature. The film is converted to PPV by heating at a temperature of 170-300°C.

After the polymer is deposited onto the ITO coated slide, aluminum contacts are evaporated on top. The aluminum contacts are masked into four mm strips which run across the length of the sample, perpendicular to the ITO contacts, giving sixteen devices with an active area of $16mm^2$ each.

Contact is made to the sample by placing a thin piece of indium on top of the metal contact. Contact is then made to the indium by means of a probe contact with a flexible tip, which is lowered until the probe is in contact with the aluminum electrode. The layer of indium is soft and protects the chromium contact from damage by the probe, prolonging the life time of the devices.

3.5 Polymer Preparation

The polymer film was formed by spin coating the polymer precursor onto the slide which was then polymerized by baking at 170-300°C.

The precursor was formed by mixing concentrated NaOH with a 0.25 M solution of the monomer (see fig 3-3 (a)), cooled to 1°C. The polymerization was quenched by addition of HCl after 5 -15 minutes [16]. The solution was dialyzed through a membrane to separate molecules of molecular weight 6000-8000, and the sample was then stored in a freezer. The precursor polymer is precipitated out with isopropyl alcohol, and dried in a stream of dry O_2 free argon gas. The polymer was washed to

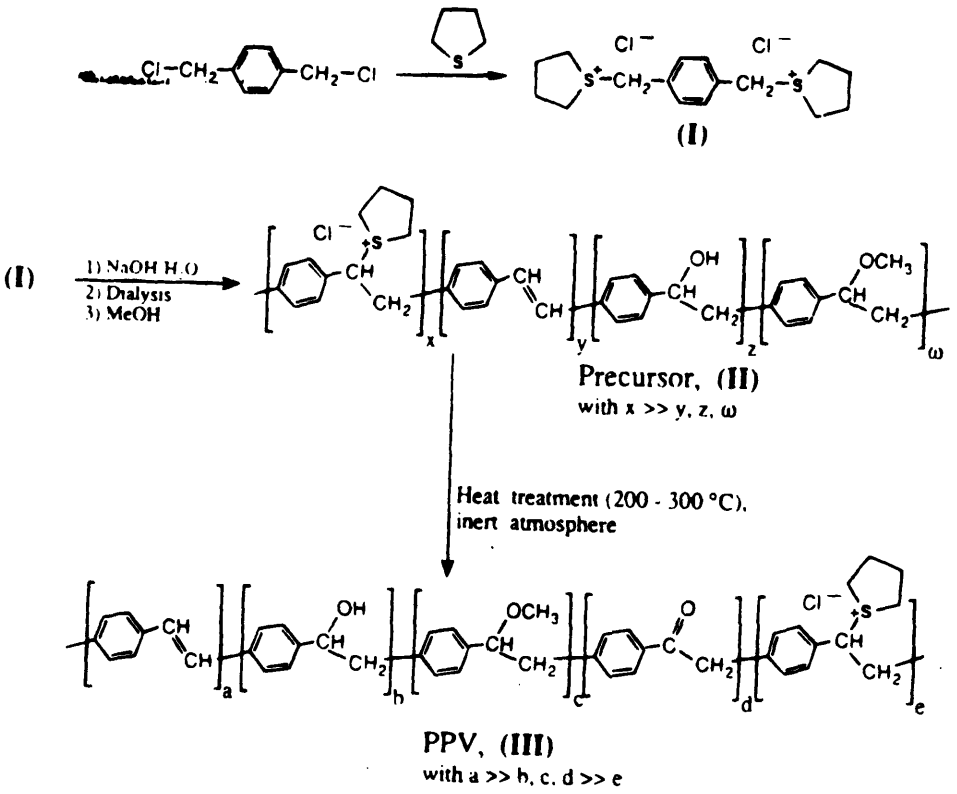

Figure 3-3: Polymer preparation. Taken from F. Papadimitrakopoulos et al., Chemistry of Materials, 1994

removed any salts.

The precursor was spuncoated on to the glass substrate. Thermal conversion was achieved by baking the slides at 170 to 300°C in a oxygen-free atmosphere. It is important that this be done in an oxygen-free environment, since the presence of oxygen leads to the formation of carbonyl groups on the polymer which act as trap sites.

The samples we used were prepared using a different precursor molecule than is normally used in PPV preparation. An advantage of using a different precursor is that the precursor we used can be dissolved in a different solvent, and hence the samples can be prepared at lower temperature. A further advantage is that the polymer has a higher percentage of cis linkages, and has an amorphous structure. There is

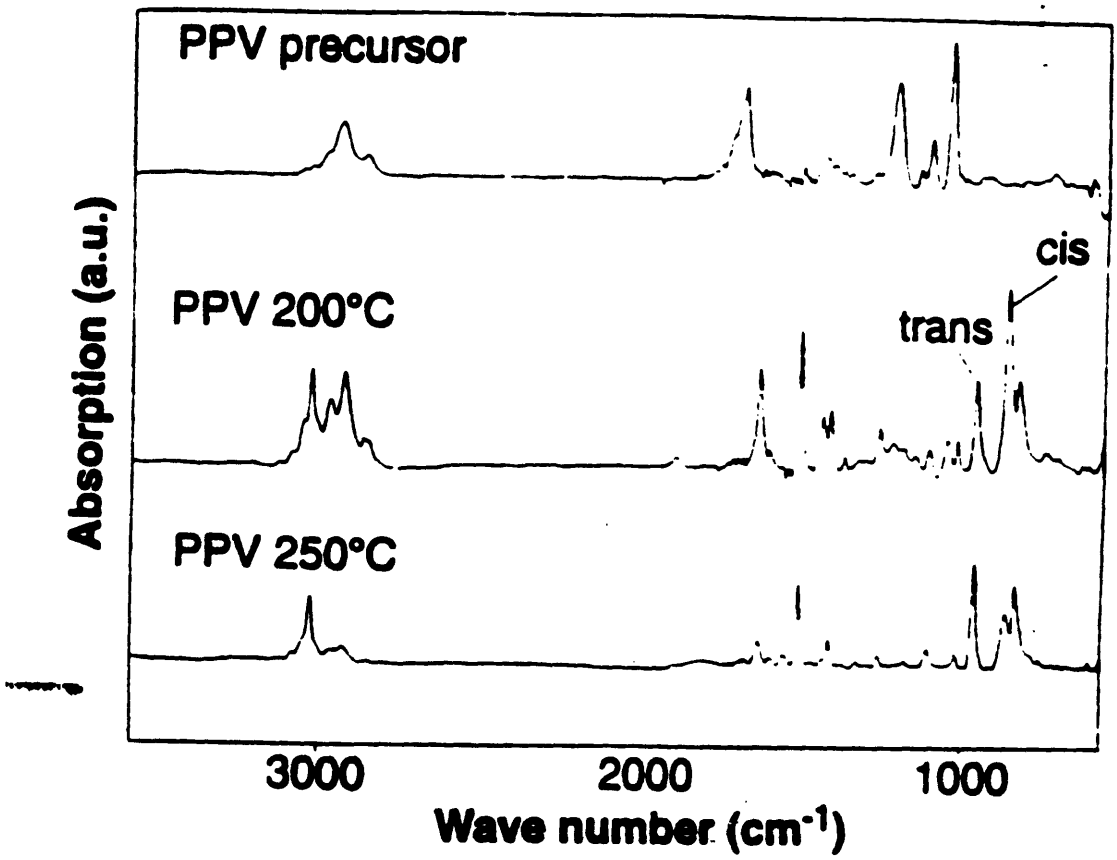

Figure 3-4: Plot of infra red absorption vs. wave number in PPV for different preparation temperatures, and corresponding to different amounts of cis linkages, taken from S. Son et al., Science April 1995
The relative amount of cis and trans linkages can be inferred by the strength of the vibrational modes in the infra red absorption spectra.

evidence [19] that amorphous PPV may have a higher electroluminescence yield, with an internal quantum yield of 0.22% [19] in comparison to an internal quantum yield of 0.01% for conventionally prepared, polycrystalline PPV.

The percentage of cis conjugation links can be controlled by changing the conversion temperature at the polymerization stage. Our samples had conversion temperatures of 170°C for the maximum number of cis linkages (and hence shorter conjugation length) and 250°C for the sample with longer conjugation length. The amount of cis linkages can be measured using infrared spectroscopy. This is shown in figure 3-4 [19].

Chapter 4

Materials and Apparatus Characterization

4.1 Absorption Spectrum

The absorption spectra of samples of PPV, with different proportions of cis and trans linkages were taken using a Hewlett Packard diode array spectrometer. The absorption spectra of the samples are given in figure 4-1(a)and (b).

The absorption spectra of the samples characterizes the relative conjugation lengths in the polymer chains. The differences in the conjugation lengths of the polymer can be measured by the blue shift of the absorption edge at 350 nm. The carriers on the polymer molecule act like particles in a box, with their energy scales being determined by the length of the box. Molecules with a shorter conjugation length will have their energy levels separated by a larger energy scale. Consequently, their absorption spectrum will be blue shifted.

The thickness of the sample, which is needed for mobility calculations can be measured from the absorption spectrum. The thickness can be measured directly using a profilometer only if the sample is quite thick. Furthermore, measuring thickness with a profilometer destroys the sample. The thickness of the sample can be extrapolated by the strength of the absorption at 300 nm, and comparing the absorption of the sample to the absorption of a very thick sample, whose thickness had been measured

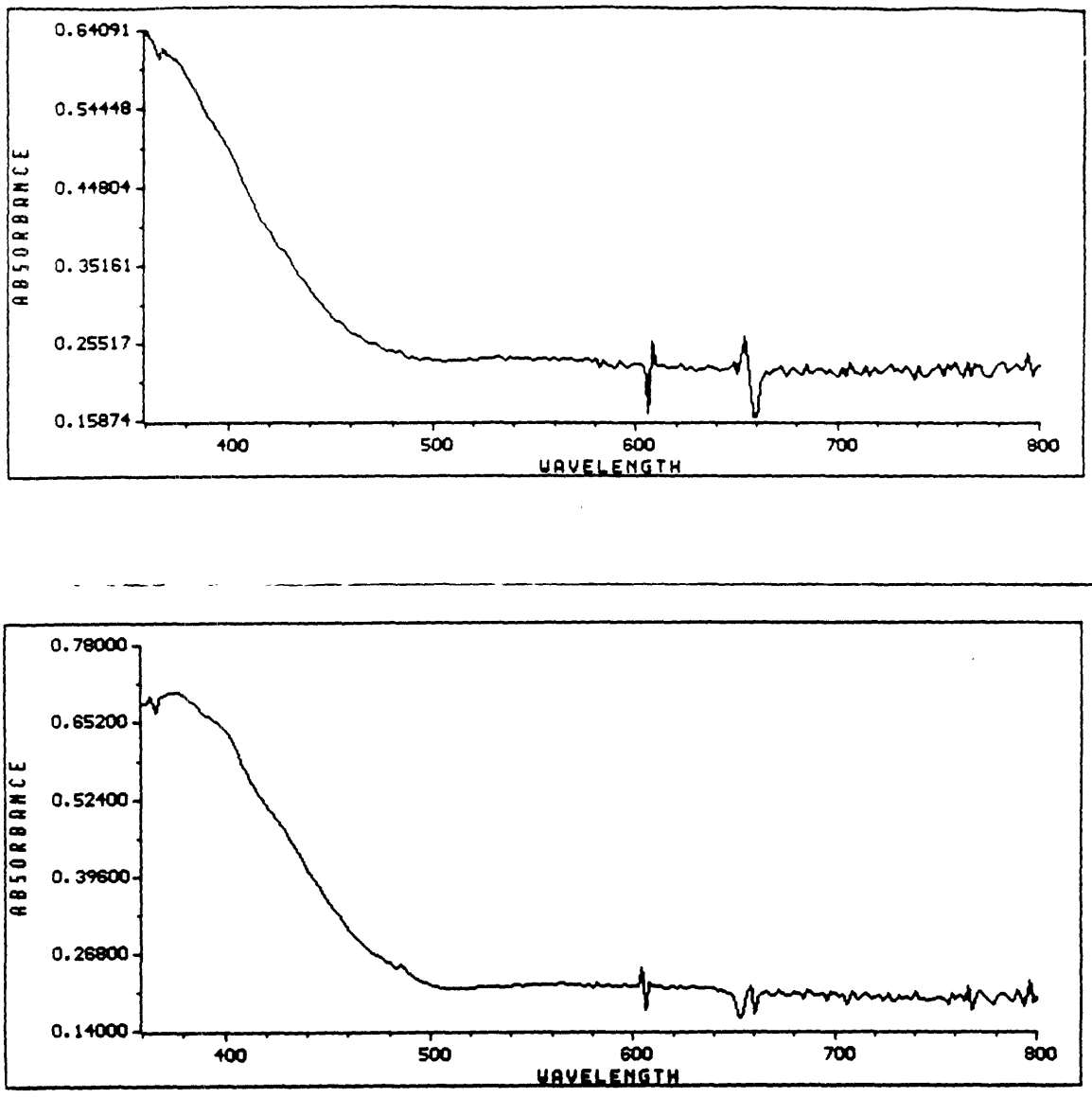

Figure 4-1: Absorption Spectra of PPV
The conjugation length of the molecules is determined by the number of cis linkages. Conjugation length can be measured by the blue shift of the absorption edge around 350 nm.

using a profilometer. The peak at 300 nm is not completely shown in the absorption spectra since it lies close to an absorption peak of glass.

4.2 Emission Spectrum

The emission spectrum of the same device was taken using a SPEX Fluorimeter. The sample was excited by a wavelength of 560 nm, and the intensity of emission was measured at different wavelengths. The peak at $520nm$ is due to the decay of the singlet state of the exciton, which is the primary emission mechanism [6].

The emission spectra of a $1000\mathring{A}$ thick sample of PPV is given in fig. 4-2, for an incident wave length of $560nm$.

4.3 Experimental Set up

The experimental setup used in the experiment is given below in figure 4-3. The signal is taken from a square wave generator with pulses at 10 Hz. The duration of the pulse is 10 ms, much longer than the RC time constant of the circuit which is 0.5 μs.

The signal is connected to the organic diode, which emits light when the voltage is applied. The light from the organic diode is collected in a photomultiplier detector. The photomultiplier is connected to a high voltage power supply of -1000V. The signal from the photomultiplier is connected to the oscilloscope with a low input impedance in order to lower the response time of the circuit (see sec 4-5).

The voltage pulse which was applied to the sample, and the light signal detected by the photomultiplier tube are displayed on the oscilloscope. The delay between the voltage pulse and the light signal is measured, and the mobility is calculated from the delay. The mobility is calculated at different field strengths.

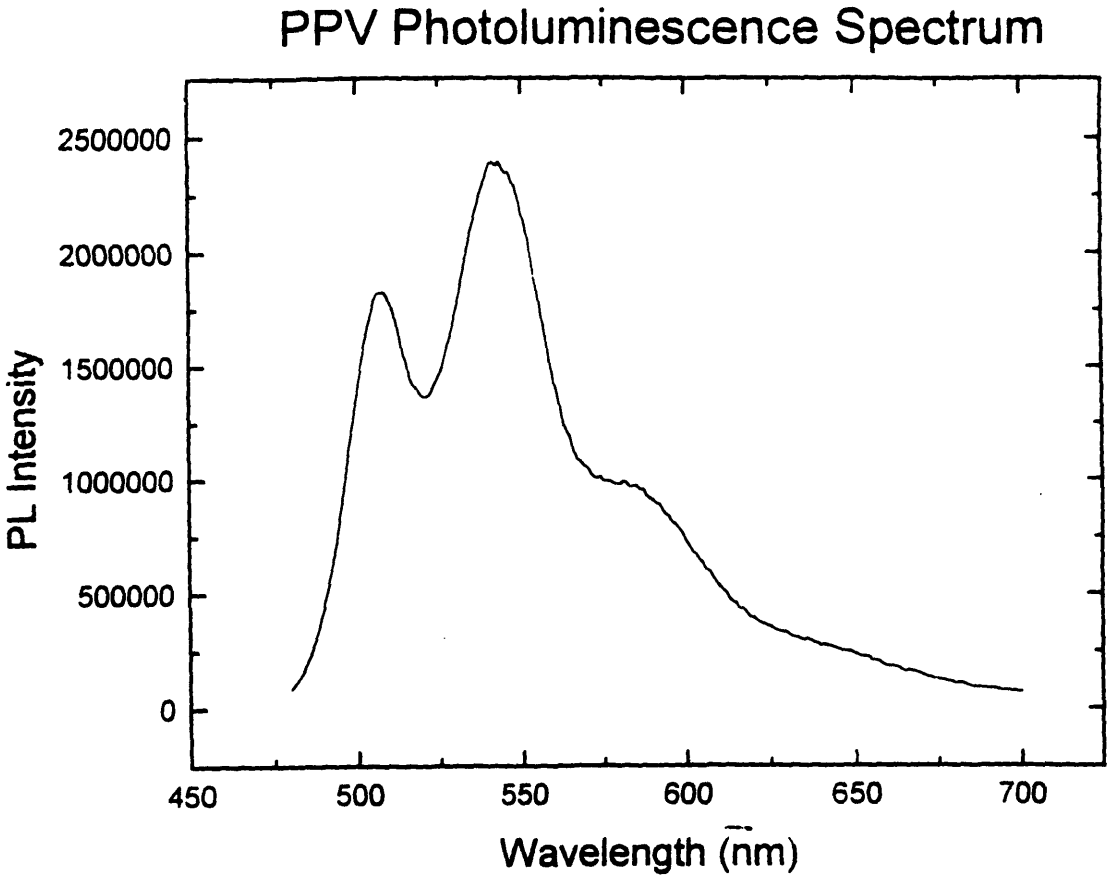

Figure 4-2: Emission Spectra for 560 nm Excitation
The photoluminescence spectrum taken for PPV has the same characteristic features as the electroluminescence spectrum.

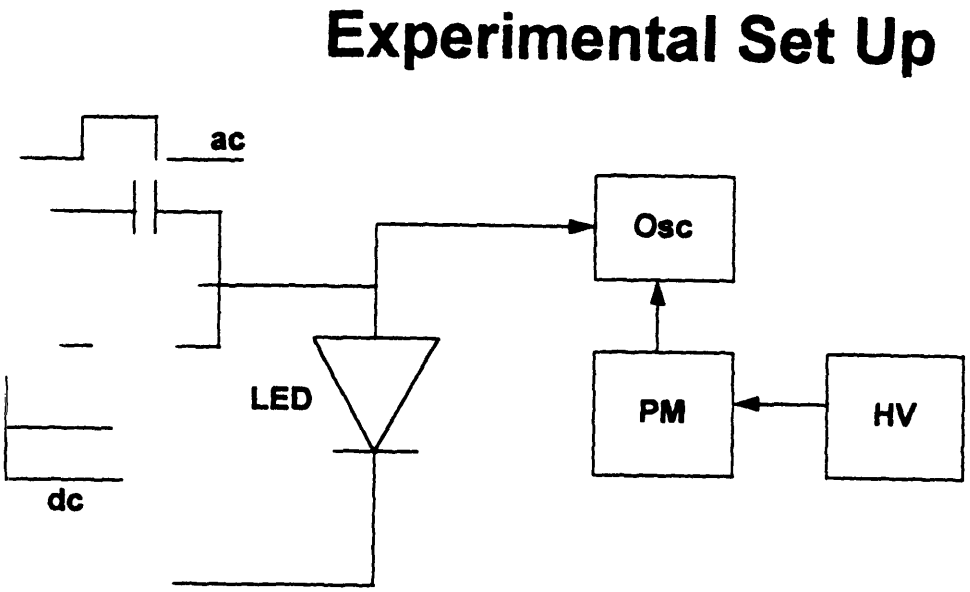

Figure 4-3: Experimental Set up
HV is the High Voltage Power Supply, PM is the photomultiplier and OSC is the oscilloscope.

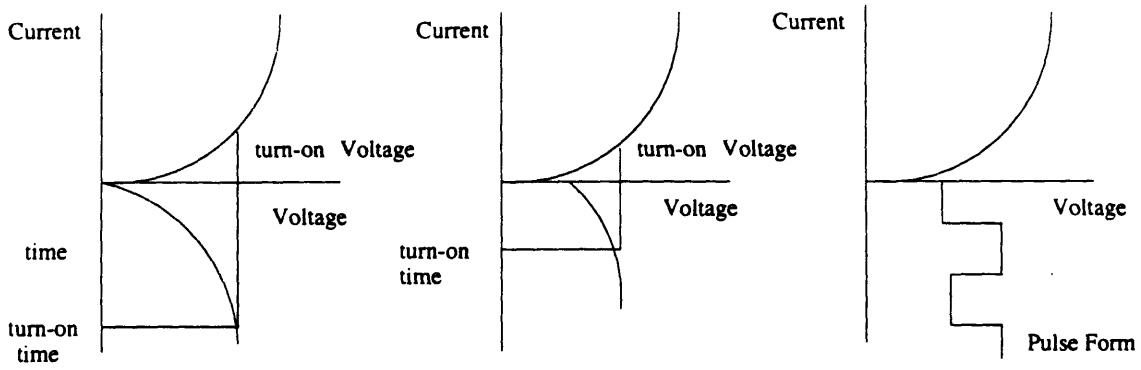

Figure 4-4: Pulse signal

Biasing the diode at a dc level close to the turn-on voltage of the diode lessens the turn-on time of the diode. This technique is important for samples with transit times which are on the order of the turn-on time.

4.4 Electrical Properties

The response time of the sample is limited by the time needed (turn-on time) to build up enough voltage across the sample for light to be emitted (turn-on voltage), and by the time resolution of the measurement circuitry (RC- time constant). If the input impedance of the oscilloscope is set to 0.5 $k\Omega$, the RC time constant is 0.4μs. In order to reduce the turn-on time for the diode, a square wave pulse of low amplitude with a dc bias can be applied. The dc bias is chosen to be immediately below the turn-on voltage of the diode. The time needed to reach turn-on voltage is reduced. The pulse signal used is shown in figure 4-4.

Using a dc offset for the pulse makes the sample degrade at a faster rate. For a sample thickness of 1000Å, it was not necessary to use a dc bias, since the drift times were much longer than the turn-on times of the sample. This technique is important for thinner samples or for samples with higher mobilities.

4.4.1 Current-Voltage relationship

The turn-on voltage of the diode can be determined by graphing the current flowing through the diode against the voltage applied across the diode. The current-voltage relationship of the diode was plotted using a Tektronix 575 transistor I-V curve tracer, with the metal electrode connected to the base connection, the ITO electrode connected to the collector, and the meter set to the pnp mode. The emitter is grounded.

The current-voltage relationship of the organic diode is given below in figure 4-5. The turn-on voltage is around 15 Volts.

4.5 Instrument Resolution

The experiment was originally performed using an inorganic aluminum gallium arsenide LED. We assume the response time of the device is instantaneous and we use the data from the inorganic diode to determine the instrument resolution of our experiment.

The experimental set up was the same as in fig. 4-3. The turn-on voltage of the inorganic diode was measured to be 1.5 V using the I-V curve tracer (see fig. 4-6), so the diode was biased at 1.5 V, with a square wave pulse of 1 V amplitude at 1 kHz.

The input impedance of the oscilloscope was controlled by connecting a 25 kΩ variable resistor in parallel with the input terminal of the oscilloscope. The rise time of the light signal was measured for different input impedances. The rise time increased with increasing impedance, indicating that the signal was limited by the instrument resolution.

A graph of the measured rise time against the termination resistance is given in fig. 4-7.

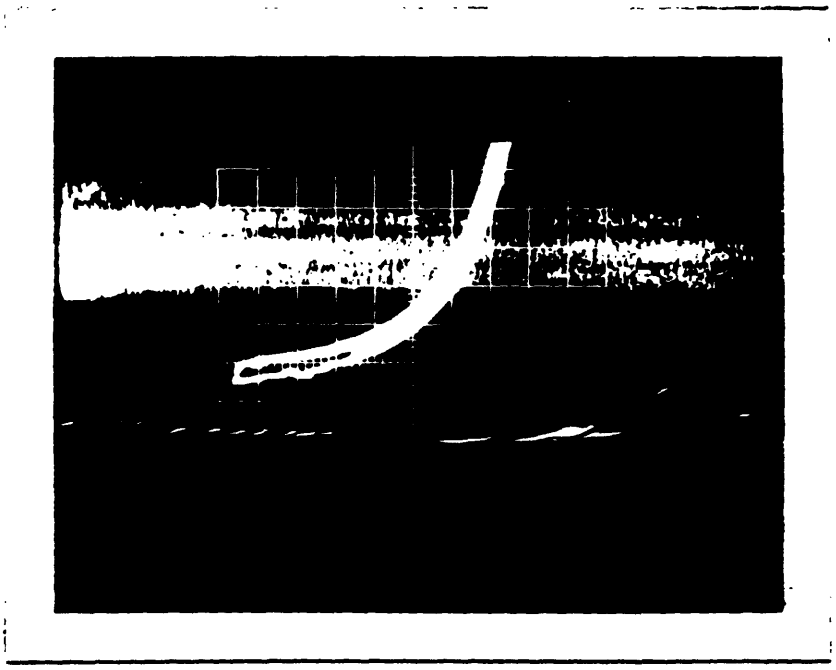

Figure 4-5: I-V curve of PPV diode
Voltage is graphed on the x-axis (5 volts/div) and current (0.05 ma/div) is the y-axis.

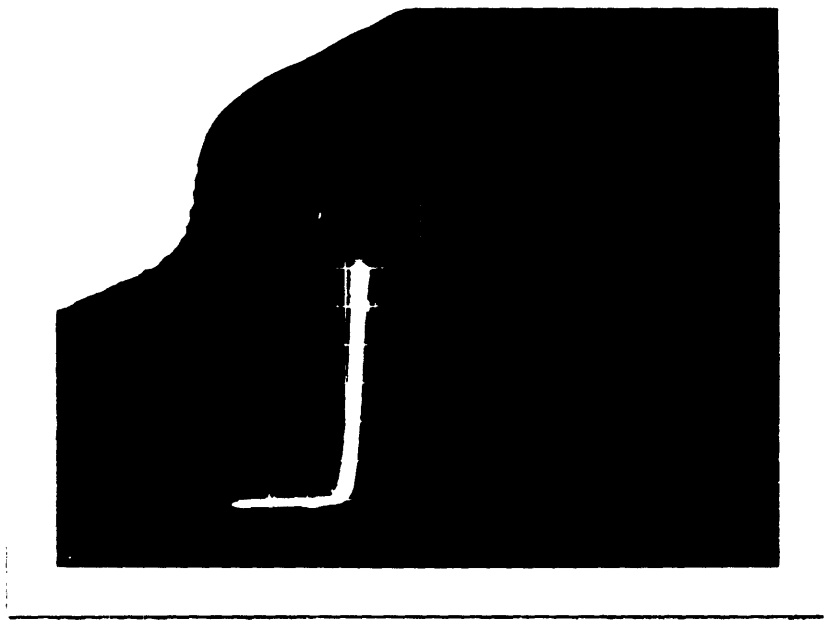

Figure 4-6: I-V trace of inorganic LED
The x-axis is voltage (.5 V/div) and the y-axis is current (.05 ma/div).

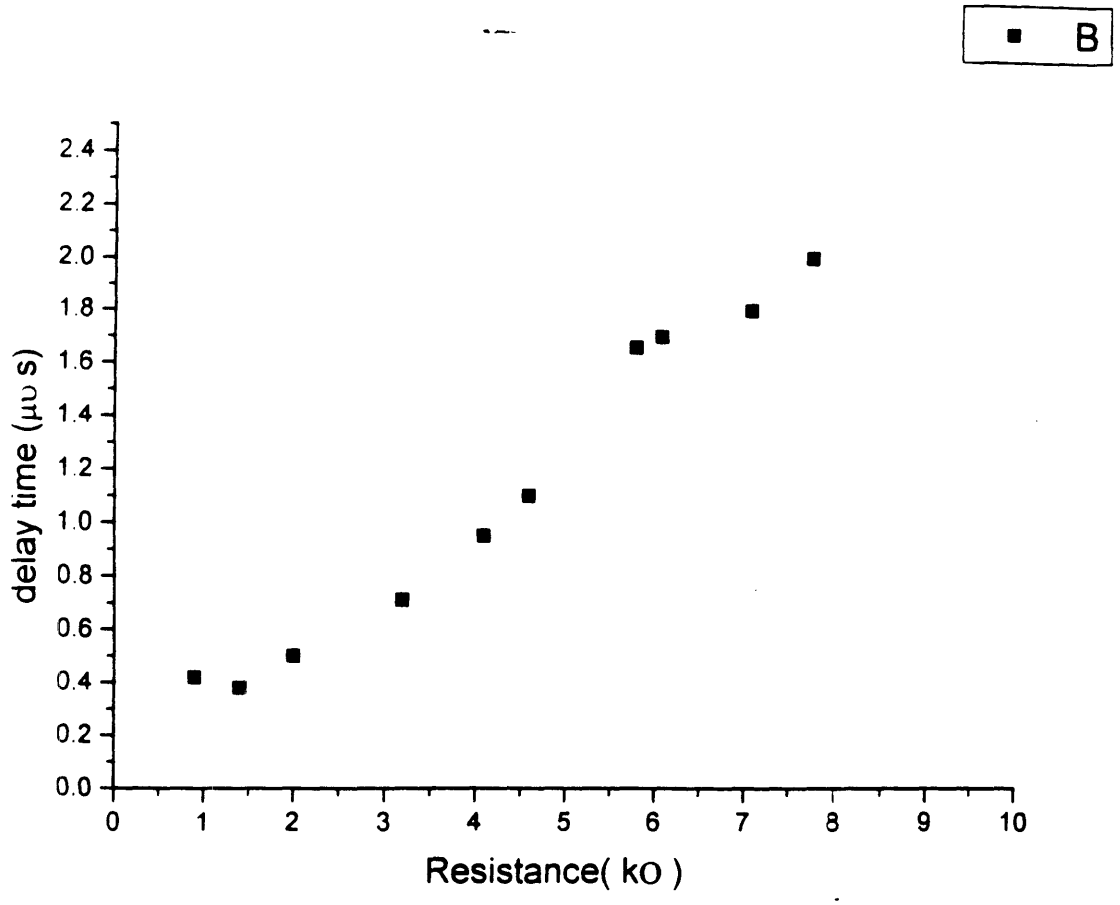

Figure 4-7: Instrument resolution
The time taken for the light signal to reach half of it's maximum amplitude is graphed against the termination resistance of the oscilloscope.

Since the organic LED has a much shorter rise time, it is possible to use a higher termination resistance with the organic LED than is used for the inorganic LED. In addition, since the light emission is lower, it is necessary to use a higher termination resistance in order to maximize the signal.

A typical mobility for an organic polymer is between $10^{-4} - 10^{-8} cm^2/Vs$. Assuming an applied voltage of 50 V, and a film thickness of 1000Å, and a mobility $\mu = 10^{-4}$, this will result in a velocity

$$v = \mu E = \mu V/d,$$

and a transit time

$$\tau = d/v = d^2/\mu V = 2\mu s.$$

The termination resistance was chosen to be 500 Ω, in order to give an instrument resolution of 400ns, which is adequate resolution for PPV samples.

4.6 Photomultiplier

A second source of delay in the circuit is the turn-on time of the photomultiplier. By increasing the voltage of the high voltage power supply, the delay time of the photomultiplier tube is decreased. In addition, if more voltage is applied to the photomultiplier, then the detection signal will have a higher amplitude, and the termination resistance of the oscilloscope can be raised even higher. On the other hand, a higher voltage means a higher noise level. In particular, the photomultiplier detector is likely to pick up more noise from the room lights in the background.

Using the inorganic LED, the effect of the high voltage supply on the rise time of the signal is measured. The delay times as a function of Voltage are shown in figure 4-8. The delay of the signal is less than the transit times we were expecting to measure when the voltage supply was in the range of -500 to -1000 V. A voltage of -1000V was chosen since the PM picked up a lot of noise from the room lights at higher voltages. The delay in the signal was $40ns$ when the voltage was set to -1000

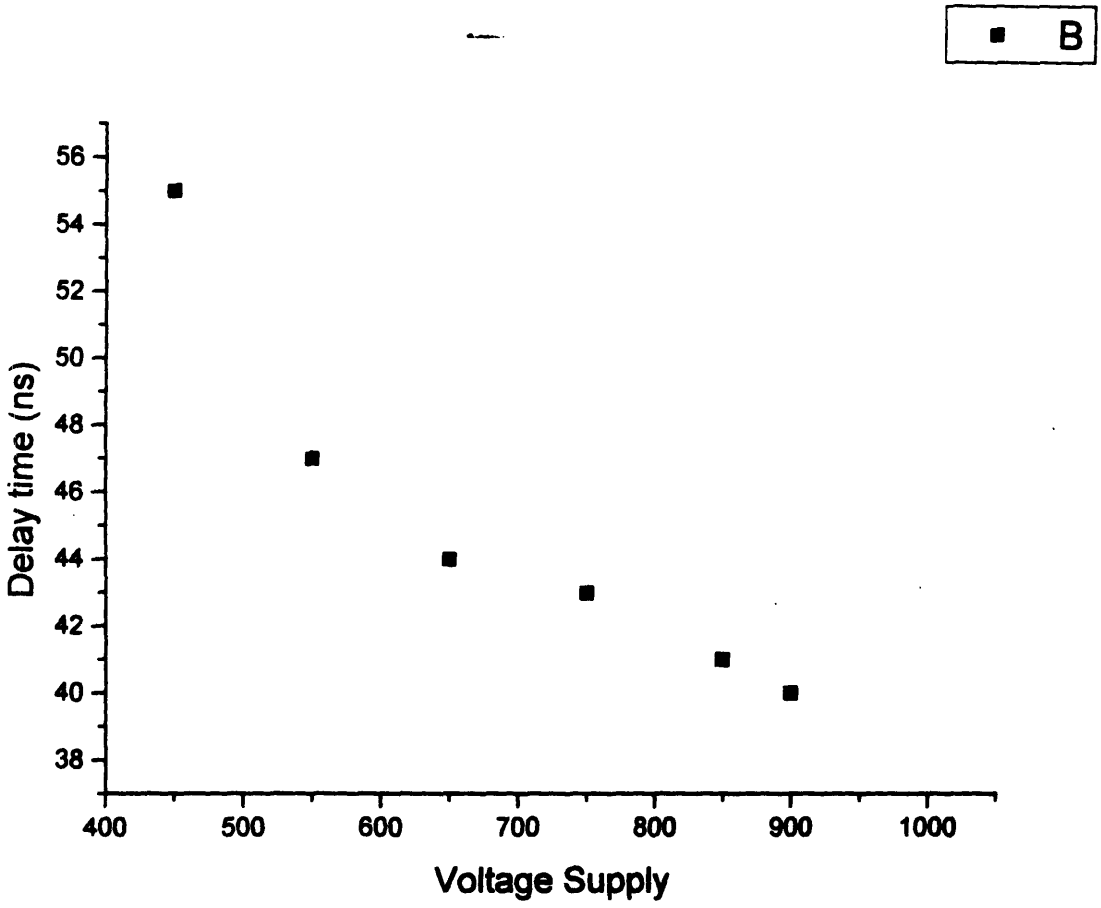

Figure 4-8: Delay time vs. PM Voltage
The effect of the Photomultiplier voltage supply on the delay in the light signal is given.

V. which is negligible compared to the instrument resolution.

Chapter 5

Results

The distribution in the mobilities was extracted from the shape of the emitted light pulse. The mean mobility obtained was lower than the mobilities which have been reported previously [1, 11] for PPV without cis-inclusions grown by the Wessling Method. These mobility measurements are based on time-of-flight photoconductivity measurements [8] for PPV in a sandwich geometry. The difference in the measured mobilities may be due to the greater prevalence of cis linkages in our sample and the more amorphous morphology of our PPV. The mobilities measured in samples with different average conjugation lengths were the same at low fields, indicating that the average conjugation length of polymer molecules does not limit carrier mobility. From the field dependence of the mobilities, it is possible to infer a trapping separation which is the same as the molecular separation.

5.1 Transit Times

Traces of the electroluminescence intensity against time are given below in figure 5-1, for a 1000$\mathring{A}$ thick sample of PPV. The data are taken for a 13 ms pulse at a 10 Hz repetition rate. The instrument resolution is 0.4μs, and the duty cycle is 10%.

It is evident from fig. 5-1 that for higher applied voltages the edge of the light signal moves to shorter times. The effect can be seen qualitatively by estimating the transit time as the time when the light signal reaches half of its maximum amplitude.

This corresponds roughly to the time when half of the carriers have traversed the sample.

5.2 Deconvolution

The mean transit time can be estimated as the time when the light signal reaches half of its maximum amplitude. However, it is also possible to extract the distribution of transit times from the light pulse. The distribution of transit times can give indications of the transport mechanisms and of dominant trap depths.

The distribution of transit times can be obtained from the detected signal of the photomultiplier tube. If all of the carriers were injected at the same time, the photomultiplier signal would be the transit time distribution. Applying a square wave voltage pulse means that carriers are injected at a constant rate over a fixed interval in time. Therefore, the contributions from each section of the voltage pulse must be included. This is equivalent to convolving the transit time distribution with the voltage pulse,

$$\begin{aligned} j(t) &= \sum_{\tau} f(t-\tau) \\ &= \int_0^t f(\tau)\Phi(t-\tau)d\tau, \end{aligned} \tag{5.1}$$

where $f(t)$ is the distribution in transit times, and $\Phi(t)$ is the pulse function

$$\Phi(t) = \begin{cases} 0 & \text{if } 0 < t < T \\ 1 & \text{otherwise.} \end{cases}$$

If the contributions to $j(t)$ for $t < T$ are taken, where T is the duration of the pulse, then equation 5-1 is equal to the integral

$$j(t) = \int_0^t f(\tau)d\tau \quad , \quad t < T$$

The transit time distribution $f(t)$ can be extracted by differentiating the signal.

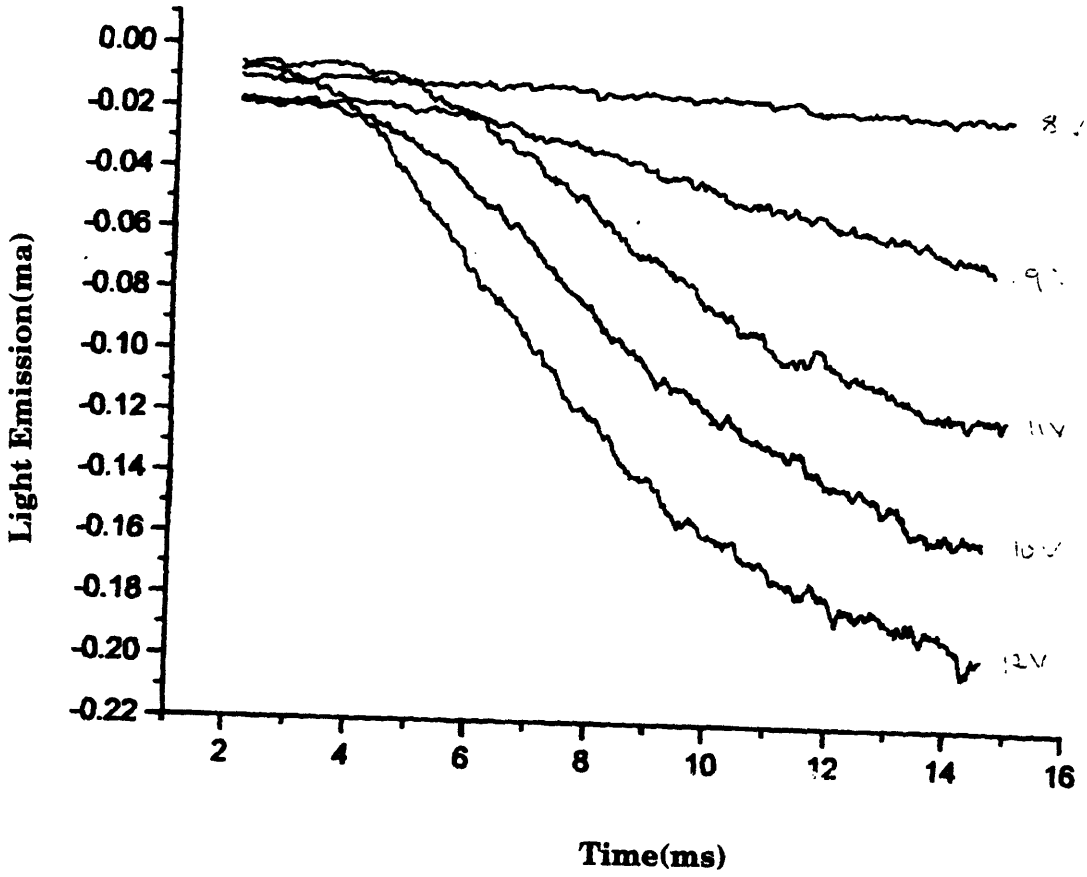

Figure 5-1: Electroluminescence signal (ma) against time (ms) for different amplitudes of applied voltage. The voltage pulse starts at 2 ms and ends at 15 ms.

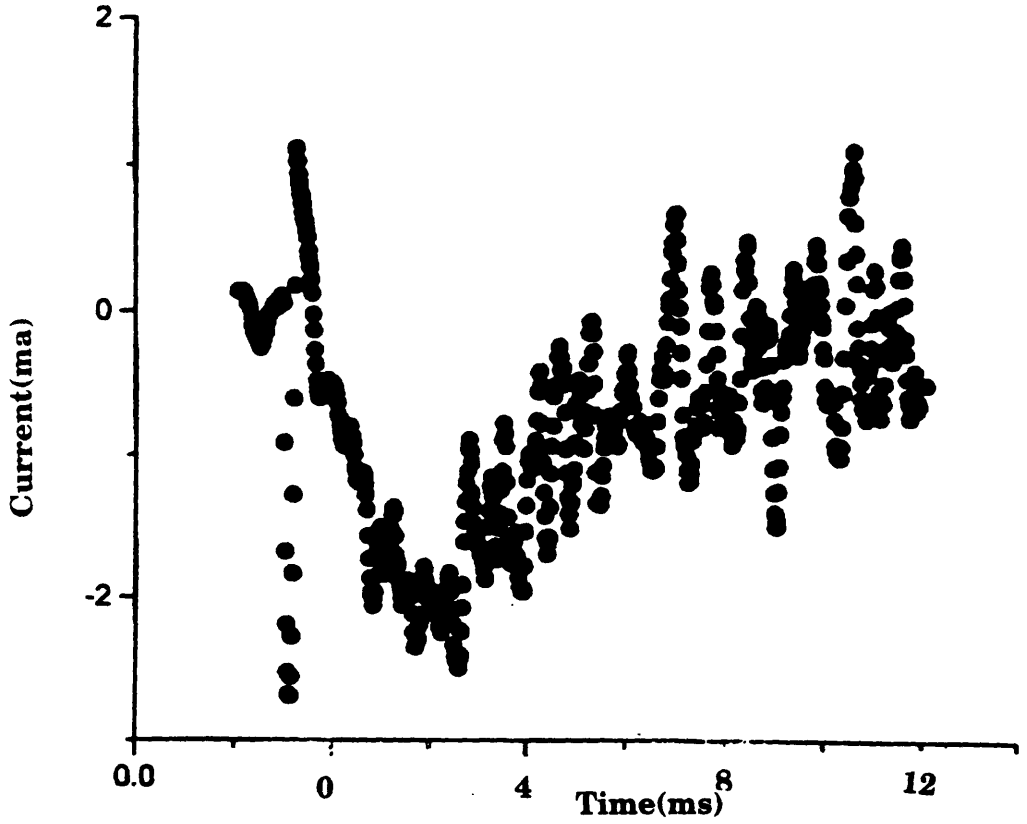

Figure 5-2: Differentiation of the light emission signal to give $f(t)$, the distribution in transit times, given as a relative probability vs. time.

The distribution of mobilities $P(\mu)$ can be extracted from the distribution in the transit times as:

$$\begin{aligned} d/\tau = \quad v \quad &= \mu E \\ \mu \quad = \quad d^2/V\tau, \\ P(\mu) = \; f(\tfrac{d^2}{V\mu}) \; &= \frac{dj}{dt}|_{d^2/V\mu} \end{aligned}$$

where d is sample thickness.

If the width of the transit time distribution is much smaller than the width of the voltage pulse, then the distribution can be extracted reasonably well. This is the case if the photomultiplier signal reaches a steady state before the pulse is turned off.

Mobility values of up to d^2/Vt', where t' is the instrument resolution of the circuit, can be resolved. Since the distribution of transit times gets cut off for transit times longer than the pulse, the mobilities which are less than d^2/VT, where T is the

duration of the pulse, cannot be resolved. With a voltage pulse of 13ms duration and a instrument resolution of 400 ns, this will enable resolution of mobilities from 10^{-4} to $10^{-9} cm^2/Vs$ for a voltage of 10 V. This gives adequate resolution for mobilities which are on the order of what is conventionally measured for PPV.

For voltages where the mean transit time is on the order of the instrument resolution, the transit time τ can be estimated as the point where the signal reaches half of its maximum amplitude.

5.3 Transit Time Distributions

The distribution of transit times extracted from our data (fig 5-2) can be compared to different analytic models to extract information about trapping mechanisms and transport properties.

The data were fitted to the analytical models derived for a single trap depth and for an exponential distribution of trapping depths. In addition, the transit times were fitted to a seventh order polynomial and a Lorentzian. By fitting the distributions to several different models, it is possible to estimate the error in the mobility which is derived from fitting the measured mobility profile to an incorrect analytical model. The mean mobility is calculated from the peak of the transit time distribution.

5.3.1 Analytic Expression

The time required for a carrier to hop out of a trap of depth E_t will follow a thermally activated distribution with the probability of hopping proportional to $e^{-E_t/kT}$.

For a single trap depth E_t, the mean transit time will be

$$\tau_0 = \frac{\int_0^\infty t e^{-E_t t/kT}}{\int_0^\infty e^{-E_t t/kT}}. \tag{5.2}$$

The distribution in transit times will be the distribution in the number of hops multiplied by the distribution in hopping times.

For an exponential distribution of trap depths, the mean transit time for each

trap depth must be averaged over the distribution in trap depth

$$\tau_0 = \frac{\sum_{E_t} \int_0^\infty e^{-E_t t/kT} t dt}{\sum_{E_t} \int_0^\infty e^{-E_t t/kT} dt} \tag{5.3}$$

Assuming an exponential distribution of trap depths, the distribution in transit times becomes [13]

$$f(\tau) = \tau^{-3/2} e^{-\tau_0/\tau}. \tag{5.4}$$

It is not possible to extract the trap depth about which the traps are distributed, since the mean transit time will depend on the density of traps as well as their depths. The integral of equation 5-3, which gives the light emission signal $j(t)$, is the error function.

A graph of the predicted distributions in transit times for a single trap depth and for an exponential distribution of trap depths is given below in figs. 5-3 and 5-4, respectively. The inverse power tail in fig. 5-3 is an artifact of the very deep traps from which the carriers cannot on average detrap. These very deep traps give rise to an increase in the background light emission.

5.3.2 Data

The distribution in transit times which we obtained was fitted to four different models for transit time distributions, the analytic solution obtained for an exponential distribution of trap depths, the analytic solution obtained for a single trap depth, a seventh order polynomial and a Lorentzian. The results for the mean transit time and the width of the distribution for an applied voltage of $10V$, and the mean mobility μ, calculated from the slope of the velocity distribution (fig. 5-5), are given in table 5-1. The data shown are for voltage pulses with different amplitudes, having a duration of 13 ms and a repetition rate of $10Hz$.

The mobilities μ calculated using the different transit time distributions differ by up to a factor of two (Table 5-1). On the basis of table 5-1, we estimate the error in μ to be a factor of two.

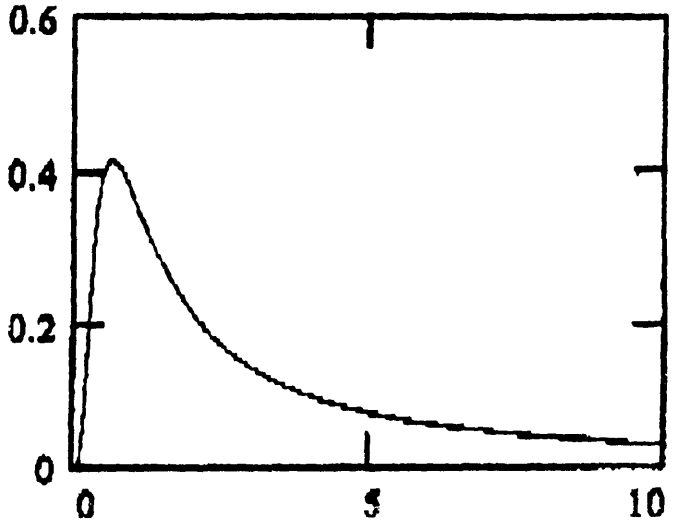

Figure 5-3: Transit time Distribution for exponential distribution of trapping depths

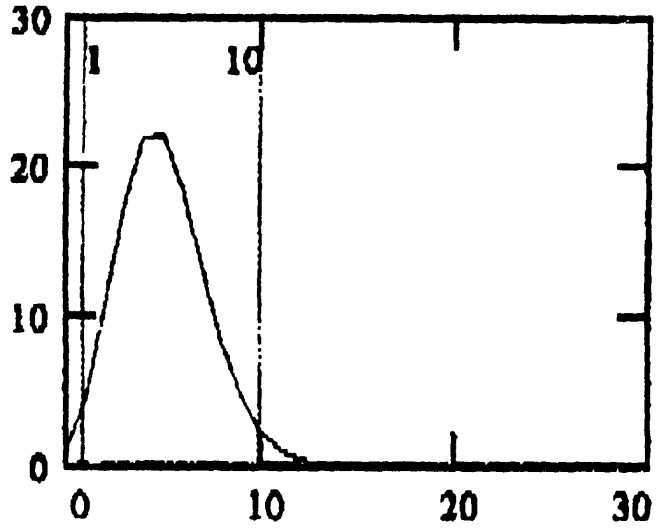

Figure 5-4: Transit time Distribution for single trap Depth

function	mean transit time (ms)	width of distribution (ms)	mean $\mu(\times 10^{-9} cm^2/Vs)$
exponential	5	3.6	4
Lorentzian	6.2	5.2	2.8
Polynomial	7.1	6	2

Table 5.1: Parameters of transit time distribution for different fitting functions The mean mobility is calculated from the slope of the mean velocity vs. voltage curve, given in fig. 5-5.

A graph of the mean velocity against voltage is given in fig. 5-5, for each of the different transit time distributions. The data did not fit the analytical model for a single trap depth well. This is partly because the single trap depth distribution will have an exponential tail (fig. 5-4). This indicates that there is no dominant trap depth in the PPV sample.

5.3.3 Mobilities

The mobility values we measured are much lower ($10^{-9} cm^2/Vs$) than the mobilities which are reported for PPV in the literature ($10^{-7} cm^2/Vs$). This is due to the different method we use to obtain mobilities, as well as to the differences in the morphologies of the samples.

The studies in the literature measure the transit time of the carriers as the time before light is first emitted (see fig. 5-6). This is equivalent to measuring the mobilities of the fastest carriers. Since the fastest carriers do not trap, this measurement may give an indication of the intrinsic mobility of carriers in the sample.

We measure the transit time of the carriers from the peak of the transit time distribution $f(t)$ (mode transit time) or as the time when the light emission reaches half of its asymptotic value (median transit time). We use the median or mode transit time since we are interested in studying trapping mechanisms, and deducing the possible trapping sites which limit the mobility. Using the median or mode transit time will give us a lower estimate for mobility than using the fastest transit time.

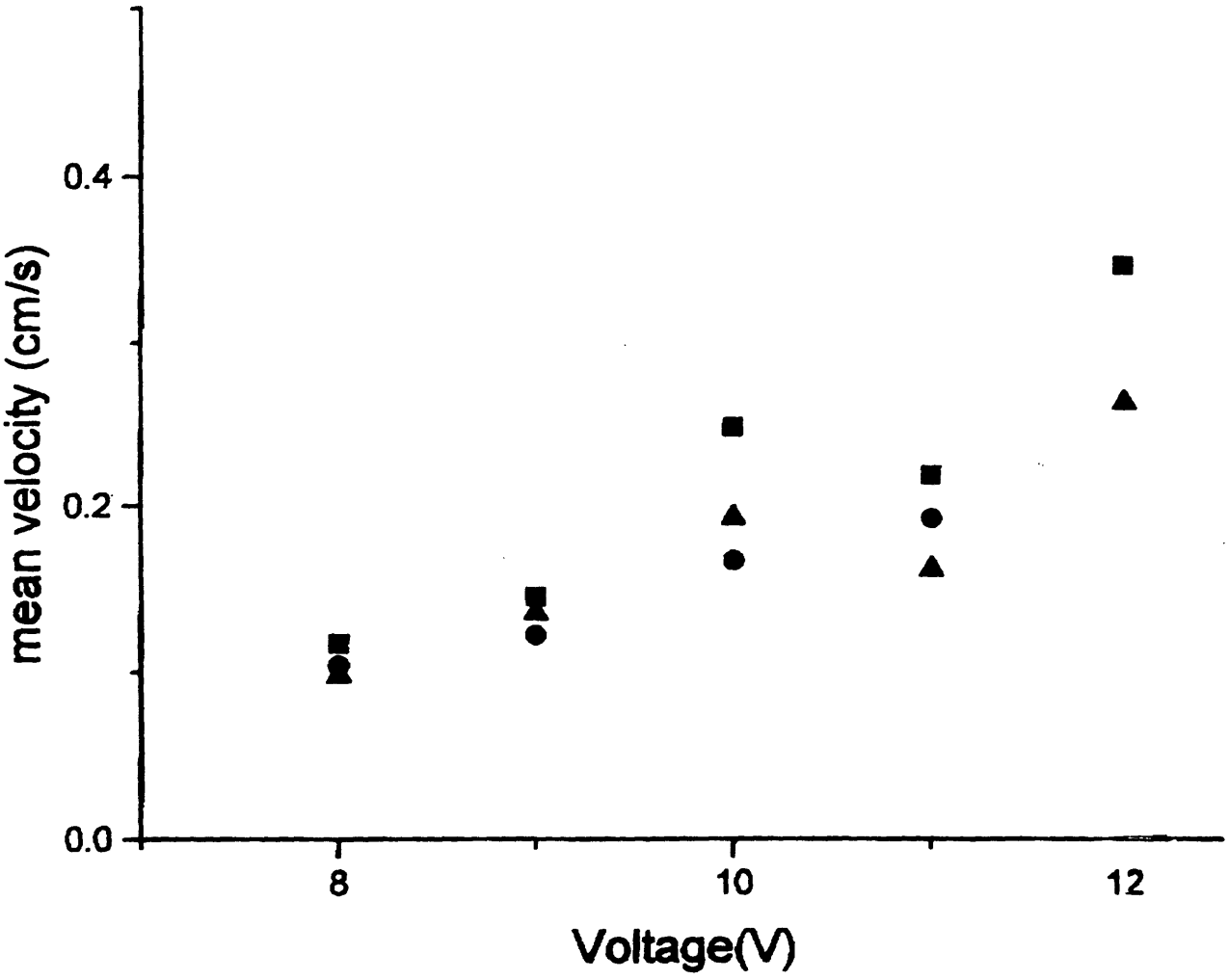

Figure 5-5: Mean Velocity Vs Voltage

The mean velocity calculated for different models is given. The mean velocity is calculated from the data for three different models, assuming the distribution of transit times follows a lorentzian distribution (triangle), a seventh order polynomial (square) or, the analytic model obtained from an exponential distribution of trapping depths (circle).

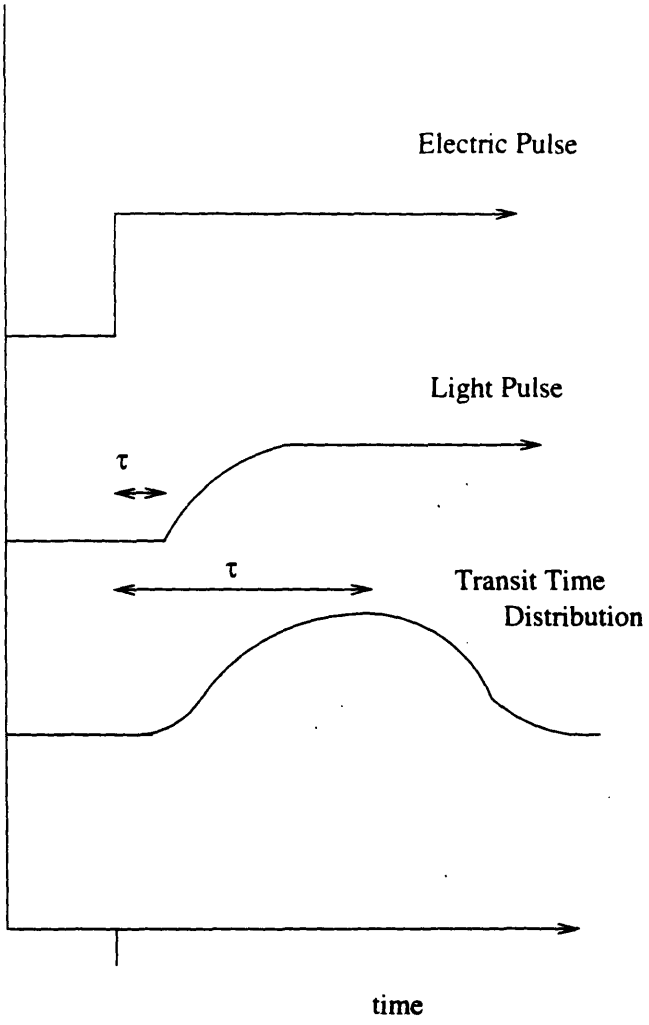

Figure 5-6: Different methods of determining transit times.
Conventionally the transit time is measured as the time when light is first emitted (top). We measure transit time from the peak of the transit time distribution (bottom). The transit time distribution is obtained by differentiating the light emission signal (see sec. 5-2).

5.4 Injection

A problem with the devices is that they degrade over time as they are used. The intensity of the light emission decreases as the devices are used. In conjunction with this, the current-voltage graphs of the devices are also altered over time. It is likely that these changes are due to the formation of metal oxide at the Aluminum contact, which increases the barrier through which the carriers have to tunnel. As a result, the current injection decreases. To check that this has no effect on the mobility measurements of the device, the electroluminescence measurements were repeated as the devices degraded. It was found that the average transit time of the carriers does not change as the light intensity decreases.

The contact potential of the devices does not change either. The contact potential is determined as the voltage which has to be applied before charge is injected, and can be measured from the I-V curves. That the contact potential did not change is an indication that the amount of voltage dropped across the bulk of the sample does not change, and hence that the mobility is constant for a constant transit time.

To analyse the change in injection mechanism with time, current-voltage graphs are taken when the sample is new, and after it has been used for 8, 20 and 30 minutes. The sample was driven with a 20 V pulse at a 15% duty cycle. The different current-voltage graphs are given in fig 5-7. It is apparent that the amount of charge injected at a constant voltage is decreasing as a function of time.

5.4.1 Fits

The I-V curves which were taken as the device degraded were digitized and were fit to equation 3-12 for space-charge limited injection, equation 3-13 for tunneling injection and equation 3-11 for thermionic injection. The I-V curves were fit in order to see whether the injection mechanism changed because of the build-up of space-charge.

The fits are given below in figure 5-8 when the device was new (a), and after 20 min (b). The functional dependence can be seen best when the data are plotted on log-log or log-linear axes. The devices are space-charge limited after they have been

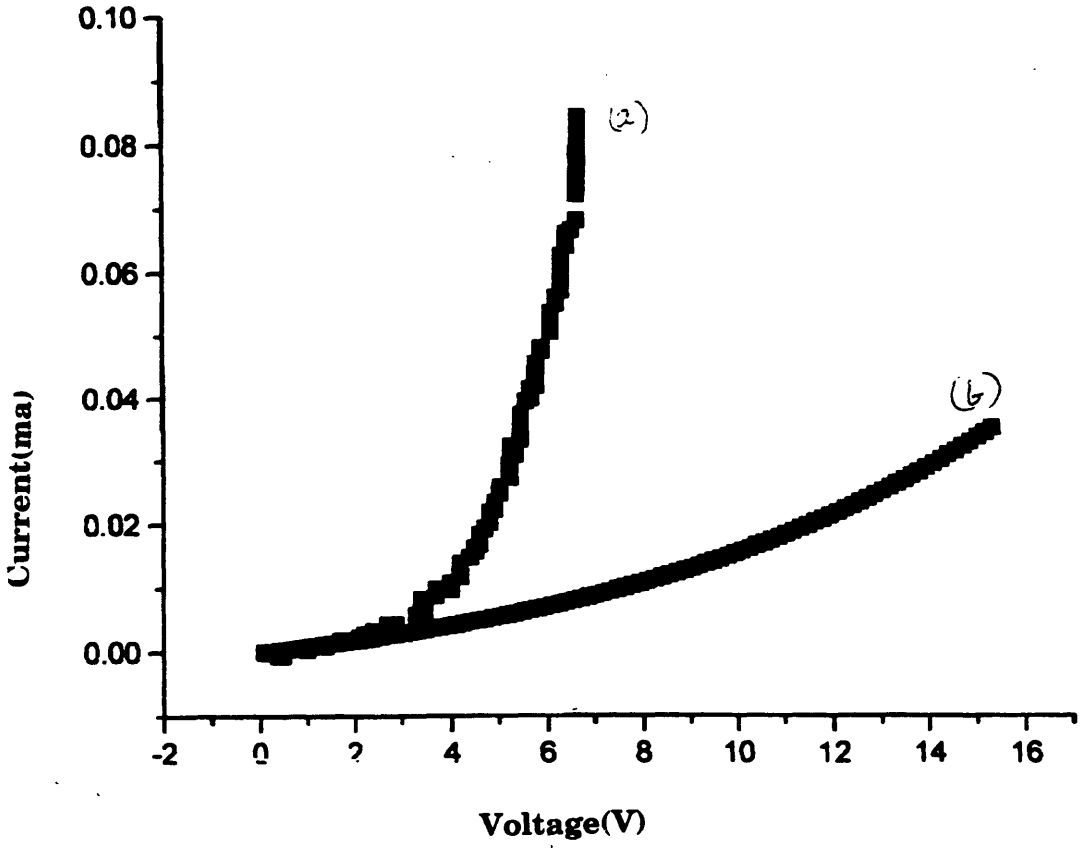

Figure 5-7: Current vs. Voltage after (a) 0 min and (b) 20 min of operation. The changes in injection levels and the changes in the shape of the I-V curve are apparent.

run for 20 min, while they are not space charge limited when they are new.

It is possible to estimate the mean carrier mobility from the fit of the I-V curve against the space charge limited model. For a value $\epsilon = 3 \times 10^{-13} F/cm$, typical of organic semiconductors, the mobility μ is $0.5 \times 10^{-8} cm^2/Vs$. This value of μ is on the order of the value which is obtained from the electroluminosity data (see Table 5-1), which is further evidence that after 20 minutes the device is space-charge limited, and that the injection rate is limiting the electroluminosity yield of the sample.

If the devices are space-charge limited, many carriers are trapped in the region about the contacts. In this region, there is a higher concentration of trapping sites where the carriers can undergo non-radiative recombination. If the devices are space-charge limited, the proportion of carriers undergoing non-radiative recombination may increase, and light emission intensity may decrease faster than injection levels decreases, as the device degrades.

We compared the decrease in injection levels to the decrease in light emission levels, and found that they both decrease at the same rate. The light emission levels were measured as the asymptotic values of the detected signal from the photomultiplier tube. The injection levels were measured from the I-V curves of the devices. This indicates that the rate of non-radiative recombination is not increasing. This result is consistent with the observation that the mean carrier mobility does not change. The carrier mobility is limited by the rate at which the carriers trap. Since the mobility does not change it is likely that the probability of trapping does not change. Non-radiative recombination occurs for particular types of trapping sites.

It seems plausible that the degradation of the sample is due to the decrease in injection rates. All of the changes in the luminosity data can be accounted for by the decrease in injection levels, and the sample becoming space charge limited. There is no evidence that the transport properties of the polymer are changing with time.

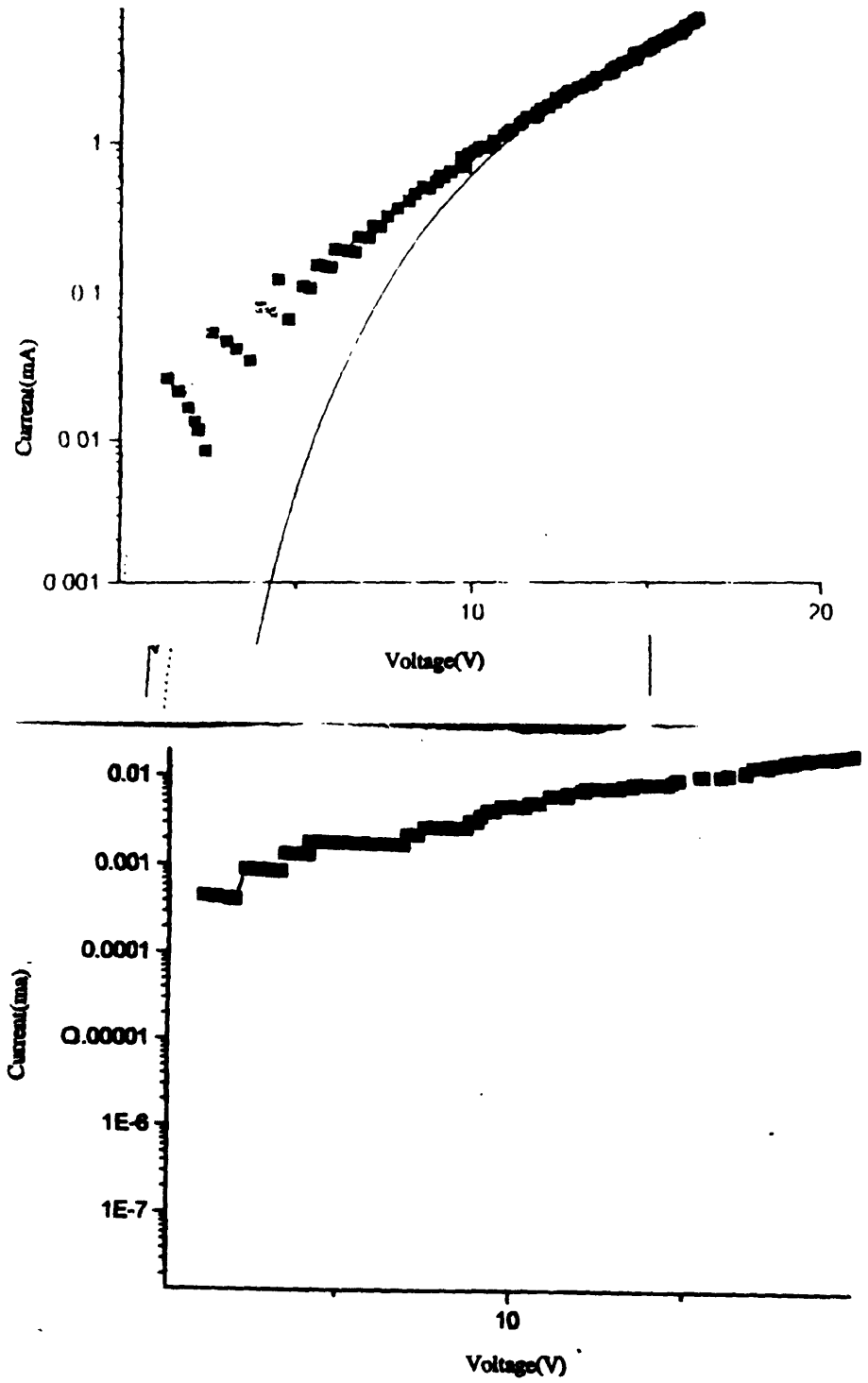

Figure 5-8: Fit of thermoionic (dotted) and space charge limited (straight) injection models for (a) new device, on log-linear axes and the same device after (b) 20 min, plotted on log-log axes

5.5 Field Dependence

The mobility was calculated for different applied voltages. Since some of the transit times were on the same order as the instrument resolution, the mean transit time was estimated as the time when the current reaches half of its asymptotic value.

The mobilities which were calculated for different applied electric fields are plotted in figure 5-9 and fig 5-10. Fig. 5-9 gives the mobilities at low field strengths, and is plotted on linear axes. Fig. 5-10 gives mobilities at high field strengths and is plotted on log-log axes. The mobilities are constant for low applied fields, and increase for fields greater than $E = 2 \times 10^6 V/cm$. This is the behavior which has been reported in studies of other organics.

The increase in the mobility which is seen is likely to be due to field dependent detrapping of the carriers. If the mobility is limited by the rate at which carriers hop between molecules, then the energy difference between molecules is $U = qdE/\epsilon = 2.8 \times 10^{-2} eV$, where E is the electric field strength, and d is the distance between molecules which can be taken to be $3 - 4\mathring{A}$. This value of U is roughly on the order of $kT = 0.025eV$, the thermal energy. Since the mobility becomes field dependent for fields which are on the order of the thermal energy, it is likely that the increase in mobility can be accounted for by field dependent detrapping.

5.5.1 Poole-Frenkel Model

If the field strength applied to the sample is high compared with the thermal energy of the sample, the electrons will start to tunnel out of traps rather than hopping out of them. Tunneling occurs when the dE/ϵ is on the order of kT/q. The Poole-Frenkel theory predicts a field dependence of

$$\mu(E) = \mu_0 e^{\frac{\Delta U - \beta_F \sqrt{E}}{kT}} \tag{5.5}$$

for tunneling transport, where ΔU is the trap depth and $\beta_F = \sqrt{e^3/\pi\epsilon_r\epsilon_0}$ is the Poole-Frenkel factor, ϵ_r is the dielectric constant of the polymer, and e is the electric

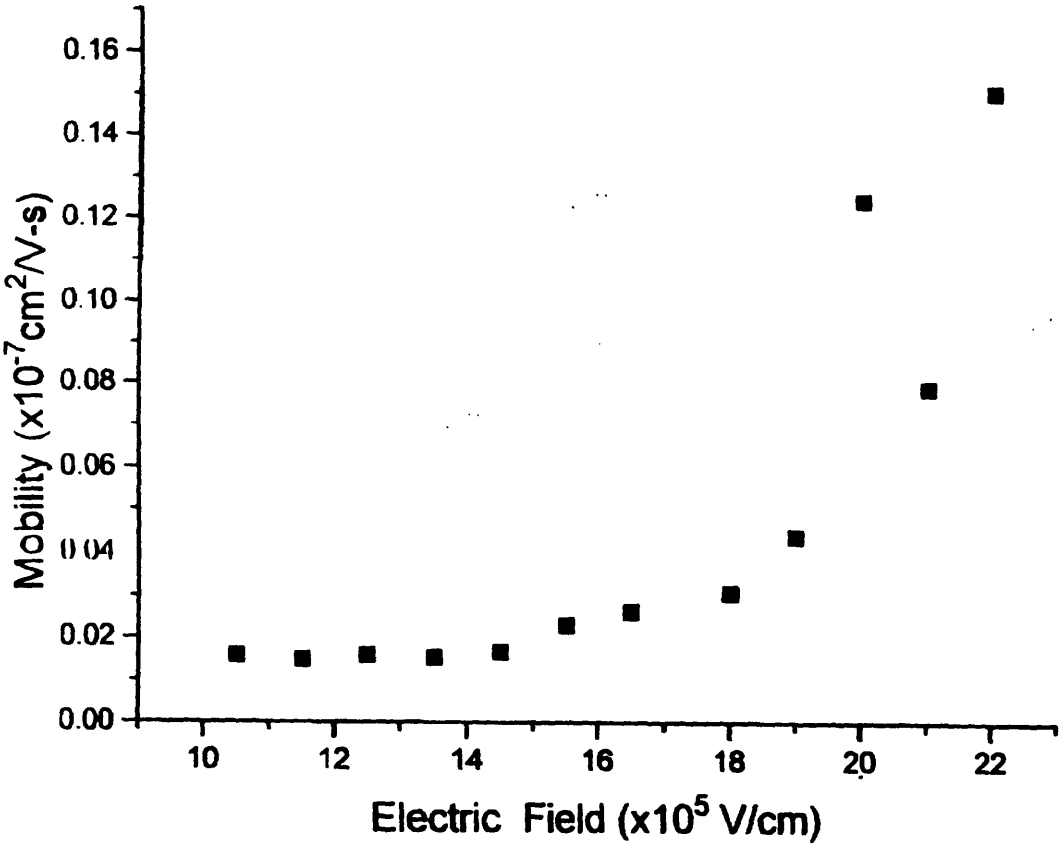

Figure 5-9: Mobility vs. electric field strength
The data are given for low electric fields. The change in mobility is seen for fields greater than $2 \times 10^6 V/cm$.

charge.

The data taken agrees with this model, as can be seen in figure 5-10. It is necessary to repeat the mobility measurements at different temperatures to obtain an estimate for the trap depths. This is planned for future work.

The mobility measured at low applied fields is lower than the mobility reported in the literature for PPV ($10^{-9} cm^2/Vs$ in comparison to $10^{-7} cm^2/Vs$ for conventionally prepared PPV). The difference in mobilities can be explained since our samples is amorphous while conventional PPV is polycrystalline. The low mobilities probably arise from the deeper traps in amorphous PPV compared to polycrystalline PPV, so that the time needed to thermally detrap is longer in our samples. It is not apparent whether the decrease in mobility is only due to the amorphous structure, or whether the decrease in conjugation length also limits the carrier mobility. This distinction is important since there are ways of preparing samples with longer conjugation lengths, for example by using longer annealing times, or for preparing samples with different packing structures, for example by changing the side groups.

If the transport is limited by the conjugation length of the sample, the energies of the molecular orbitals would be disrupted by a higher energy at the cis linkage (fig 5-11). If carriers on the molecular orbitals act like particles in a box, then the energy levels are determined by the conjugation length of the molecules. Examining the temperature dependence of the trapping will give a value of ΔU, the trap depth. Whether or not the conjugation length of the molecules limits transport can be determined by whether the measured trapping energies scales with conjugation length, and whether the trapping energies are of the same order (tenths of eVs) as the traps which would result from hopping between conjugation links. This is planned for future work.

5.6 Polymer orientation

The mobilities which were extracted from the samples were lower than the mobilities reported in the literature. We attributed these differences to the increased amount of cis- conjugation links in the sample and to the amorphous nature of the mate-

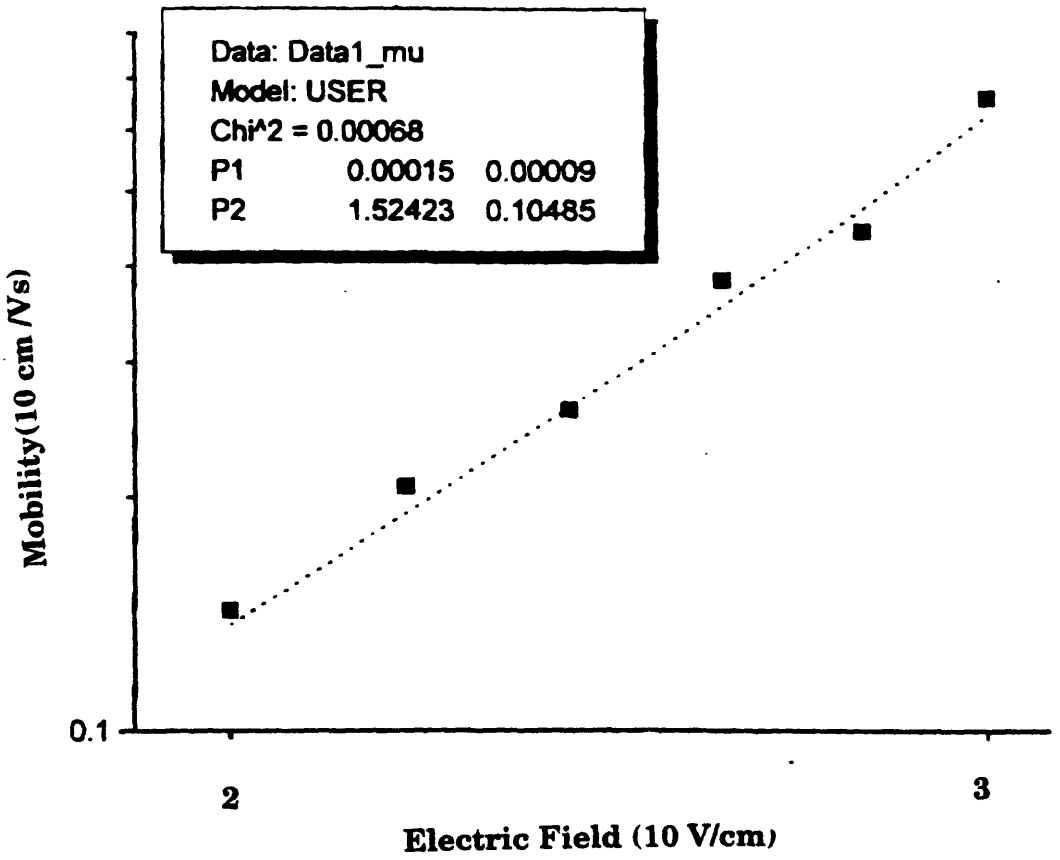

Figure 5-10: Mobility vs. electric field for high field strengths
The fit is to the Poole-Frenkel relation given in eq 5-5, the data are plotted on log-log axes.

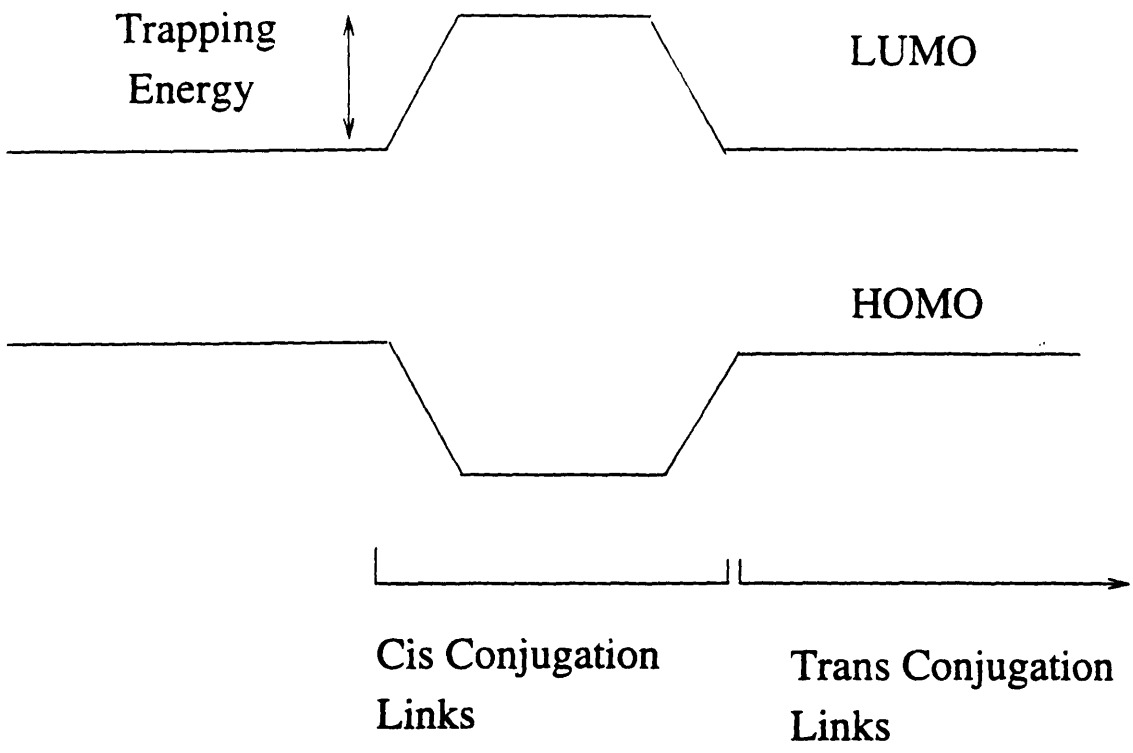

Figure 5-10: Molecular Orbital Levels with cis linkage
The trap depth is an artifact of the higher energy gap between molecular orbitals in the cis linkages.

rial. To test whether the conjugation length of molecules limits mobility values, we repeated the analysis, with a sample which had been prepared using the same precursor molecule, but which had been annealed at a higher temperature, and which had a longer conjugation length. The relative conjugation length of the molecules can be measured by the position of the absorption edge near 350 nm (see fig. 4-1).

5.6.1 Electric Field

The mobility of a sample with a longer conjugation length was calculated using electroluminescence data. The graph of the mean mobility at different electric field strengths are given in figure 5-12, for low electric fields and in fig. 5-13 for high electric fields. The mobility values follow the same pattern, with the mobility being constant at low fields ($\mu = 2 \times 10^{-9} cm^2/Vs$) and increasing above a field strength of $1.4 \times 10^6 V/cm$.

The mobility of the sample with longer conjugation length molecules is roughly constant at low voltages, and has the same value at low voltages as the sample with shorter conjugation length molecules($\mu = 2 \times 10^{-9} cm^2/Vs$), which indicates that conjugation length does not limit the mobility of the samples.

The dependence of the mobility on field strength fits the Poole-Frenkel model well. The mobilities in the second sample become field dependent at a lower electric field. This is what is expected if the mobility were limited by the time taken to hop between conjugation links. If this were the case, the longer conjugation links would mean a longer distance between hopping sites. Consequently, the mobility would become field dependent at a lower electric field.

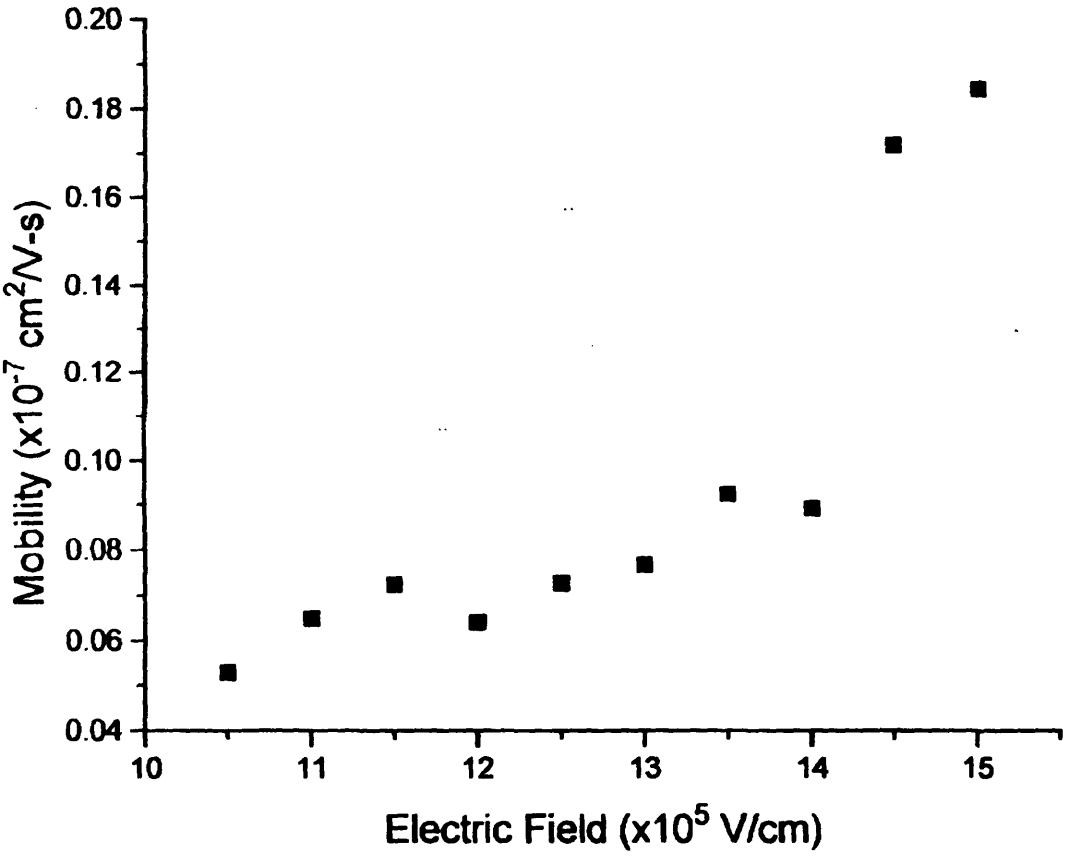

Figure 5-12: Mobility as a function of electric field for longer conjugation length molecules
The data are given for low electric fields. The mobility becomes field dependent for fields greater than $1.4 \times 10^6 V/cm$

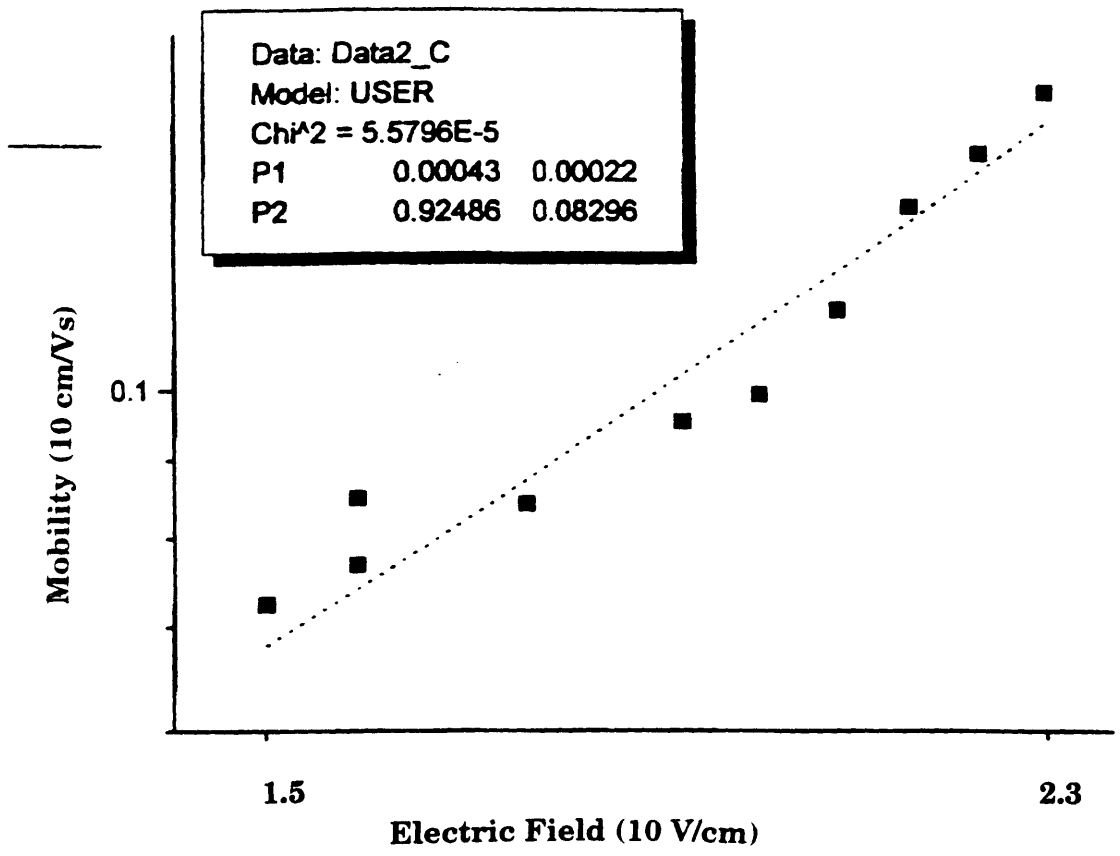

Figure 5-13: Poole-Frenkel fit of mobility vs. field strength for high electric fields, and a longer conjugation length
The data are shown for high electric fields on log-log axes. The fit is to the Poole-Frenkel model given in eq. 5-5.

Chapter 6

Summary

The use of organic polymers as active elements in transistors or light emitting diodes is motivated by their compatibility with plastic substrates, and the ease with which they can be manufactured. To this end, new production methods are being investigated which enable polymer production at lower temperatures. The polyphenyl vinylene (PPV) sample on which our measurements are based was produced using one of those new techniques. By using a precursor which could be dissolved in a different solvent, the conversion temperature was lowered, and the polymer was compatible with more plastics. This method was used because it produced a polymer with a large number of cis linkages. Including cis linkages in the polymer means that the PPV has an amorphous structure instead of a polycrystalline structure. There have been suggestions that using amorphous PPV may increase the luminosity yields of the devices [19].

This thesis examines the effects of the cis inclusions on the mobility of PPV. Cis inclusions affect the mobility of the sample in two ways. Firstly, the cis inclusions decrease the conjugation length of the molecule. Secondly, the cis inclusions affect the efficiency with which the molecules pack and prevent the formation of a crystal structure.

We find that the mobility of our samples is lower than that of PPV prepared in the conventional way by a factor of 100; however, this mobility is not lower for samples with a longer conjugation length. The conjugation length can be measured from the

blue shift of the absorption edge in the absorption spectrum of the sample.

The low mobility limits the luminosity yields of the devices. From the I-V curves of the device, it is evident that the charge injection is space charge limited and that the low injection levels limit the luminosity yields of the devices.

In this thesis, we also extract a distribution of mobilities from the electroluminescence measurements, and compare the experimental results to the predicted mobility distribution based on an exponential distribution of trapping depths. Our experimental data fits the predicted relation for an exponential trap distribution better than that of a single trap depth. This indicates that there is no single dominant trapping mechanism in the sample, which is consistent with the result that the mobility is not limited by the average conjugation length of molecules.

Lastly, the thesis shows that the transport properties of the devices are limited by the rate at which carriers hop between different polymer molecules, since the mobilities become field dependent for field strengths where dE is on the order of kT, indicating that the trapping site separations (d) are the same as the separations of the polymer molecules.

The temperature dependence of the mobility is expected to give an indication of the energies of dominant trapping mechanisms. It is expected that the temperature dependence of the mobilities can be fitted to a Poole-Frenkel relationship to give a value for the energy depths of the traps. Knowing the energy scale, it would then be possible to infer what the possible trapping mechanisms may be. Future work on the material includes these temperature measurements.

The PPV preparation was chosen in order to give a sample with higher luminescence yields [19]. This analysis shows that although the amorphous structure increases the luminescence yields, the low mobility limits injection rates. Still, the devices are brighter when both these factors are considered, making the technique important for LED technology.

Bibliography

[1] H. Antoniadis and E. A. Schiff, *Isotropy of drift mobility in hydrogenated amorphous silicon* Phys. Rev. Letter, **44, 8**,265 ,1991

[2] Ashcroft and Mermin Solid State Physics

[3] B. Ya. Balagurov and V. G. Vaks, Sov. Phys. JETP, **38**, 968, 1974

[4] D. D. C. Bradley Synthetic Metals *Conjugated polymer electroluminescence* **54**, 401, 1993

[5] J. H. Burroughes et al., Nature, **347**, 539, 1990

[6] C. Duke and L. Schein. Physics Today, *Organic Solids, is Energy Band Theory enough?*, **42**, Feb 1980

[7] F. Garnier, et al., J. Am. Chem. Soc. **115**, 8716, 1993

[8] J. R. Haynes and W. Schockley, *The mobility and life of injected holes and electrons in Germanium*, Phys. Rev., **81, 5**, 159, 1951

[9] A. J. Heeger et al., Synthetic Metals, *Carrier injection into semiconducting polymers: Fowler- Nordheim field-emission tunneling*, **67**, 23, 1994

[10] W. Helfrich and W. G. Schneider, J. Chem. Phys., **44**, 2902, (1966)

[11] S. Karg, PhD Thesis, University Bayreuth, 1995

[12] B Movaghar, *Theory of conduction in molecular solids- Theory* J. Molecular Electronics Vol 3, 1987

[13] B. Movaghar, *Theory of conduction in molecular solids- Applications* J. Molecular Electronics, Vol 4, 79, 1988

[14] G. V. Neudeck, Modular series on solid state devices, **Vol 2**. *The PN junction diode*, Addison-Wesley 1989

[15] L. Onsager, Phys Rev., **54,** 554. 1932

[16] F. Papadimitrakopoulos et al., Chem. Materials *The role of carbonyl groups in photoluminscence of Polyphenyl vinylene*, **6, 9**, 1563, 1994

[17] M. Silver, G. Schoenherr and H. Baessler, Phys. Rev Letters,**Vol 48 No. 5**, 352, 1982

[18] H. Scherr and E. Montroll, Phys. Rev. B, *Anomalous transit time dispersion in amorphous solids*, **Vol 12, No. 6**, 1455, 1975

[19] S. Son et al., Science, **269**, 376, July 1995

[20] Sze, Physics of Semiconductor Devices, Wiley- Interscience, 1981

[21] Y. Wang, Letter to Nature, **356**, 585, 1992